Title page

Title: High-altitude hypoxia exposure inhibits erythrophagocytosis by inducing macrophage ferroptosis in the spleen

Running title: Hypobaric hypoxia induces splenic ferroptosis

Type of article: Research article

Authors: *Wan-ping Yang*[1△], *Mei-qi Li*[1△], *Jie Ding*[1], *Jia-yan Li*[1], *Gang Wu*[2,3], *Bao Liu*[2,3], *Yu-qi Gao*[2,3], *Guo-hua Wang*[1,4]*, *Qian-qian Luo*[1]*

[△]These authors contributed equally to this work.

Affiliations:

[1]Department of Physiology and Hypoxic Biomedicine, Institute of Special Environmental Medicine and Co-innovation Center of Neuroregeneration, Nantong University, 9 Seyuan Road, Chongchuan District, Nantong, Jiangsu 226019, China.

[2]College of High-Altitude Military Medicine, Institute of Medicine and Hygienic Equipment for High Altitude Region, Army Medical University, Chongqing 400038, China.

[3]Key Laboratory of Extreme Environmental Medicine and High-Altitude Medicine, Ministry of Education of China, Chongqing 400038, China.

[4]Department of Neurosurgery, Southwest Hospital, Army Medical University, Chongqing, Chongqing 400038, China

*Corresponding author: Guohua Wang, Email-address: wgh036@hotmail.com, ORCID: 0000-0002-4810-8534; or Qianqian Luo, Email-address: qianqianluo@ntu.edu.cn , ORCID: 0000-0001-8302-3117.

Abstract

This study investigates the role of the spleen and splenic macrophages in the development of high-altitude polycythemia (HAPC), a condition characterized by an imbalance between erythropoiesis and eryptosis imbalance, typically observed in high-altitude (HA) environments. We employed a mouse model subjected to hypobaric hypoxia (HH) to simulate the conditions of a 6000 m HA exposure. For *in vitro* examination, primary splenic macrophages were treated with 1% hypoxia. Our findings revealed that the HH treatment enhanced erythropoiesis, resulting in erythrocytosis, with marked splenic contraction evident, later progressing to splenomegaly over a 14-day period. HH exposure also impaired the ability of the spleen to process red blood cells (RBCs), predominantly due to a decrease in splenic macrophages within the red pulp. Furthermore, the application of HH treatment over 7 and 14-day intervals resulted in increased iron mobilization and onset of ferroptosis within the spleen, as corroborated by the expression of iron metabolism-related and ferroptosis-related proteins. The expression levels of these proteins mirrored gene expression levels in human peripheral blood mononuclear cells. Subsequent single-cell sequencing of the spleen demonstrated a substantial decrease in macrophages 7 days post-HH exposure. *In vitro* investigations confirmed the decline in primary splenic macrophages and induction of ferroptosis following hypoxic treatment, which were reversed by pre-treatment with the ferroptosis inhibitor ferrostatin-1. In summary, the data suggested that HH exposure instigates splenic ferroptosis, predominantly in the red pulp, thereby hampering the RBCs clearance in

the spleen. This leads to increased RBCs retention within the spleen, triggering splenomegaly, which may potentially foster continuous RBCs production and accelerate HAPC progression. The major conclusion from this study elucidates the critical role of spleen and splenic macrophages in the pathogenesis of HAPC.

Keywords: High altitude, Hypobaric hypoxia, High-altitude polycythemia, Spleen, Eryptosis, Ferroptosis

Background

A plateau is a special environment characterized by low atmospheric pressure and low partial oxygen pressure. Long-term exposure to plateau environments may lead to chronic mountain disease [1]. High-altitude polycythemia (HAPC) is a common and widespread chronic mountain sickness characterized by excessive erythrocytosis [2]. Hypobaric hypoxia (HH) is the main cause of erythrocytosis, which in turn alleviates hypoxic conditions in tissues under high-altitude (HA) exposure [3]. In a healthy organism, a balance is maintained between erythropoiesis in the bone marrow and eryptosis in the spleen [4]. Even though HA/HH exposure can disrupt the equilibrium between RBC formation and clearance, healthy individuals can swiftly establish a new physiological RBC steady state [5]. However, in patients with HAPC, RBCs homeostasis is disrupted, failing to reach a state of equilibrium, which ultimately leads to a persistent increase in RBCs [4]. It is well-established that exposure to HA/HH can induce erythropoiesis, yet the pathogenesis of eryptosis under these conditions remains poorly understood.

"

The spleen plays a crucial role in maintaining erythropoietic homeostasis by effectively clearing impaired and senescent RBCs from circulation [6]. Particularly, red pulp macrophages (RPMs) within the spleen, serving as primary phagocytes, are responsible for clearing senescent, damaged, and abnormal erythrocytes from circulation to recycle iron [7]. RPMs initiate the process of RBC endocytosis and lysosomal digestion into heme, following the recognition of the RBCs earmarked for removal via their cell surface signals [8, 9]. Subsequently, heme oxygenase-1 (HO-1) decomposes the heme into biliverdin, carbon monoxide, and iron [10]. Most of the iron recycled from heme is transported out of the cell through a protein called ferroportin (Fpn). This iron then binds to transferrin (Tf), a plasma protein that transports iron in the blood. The iron-transferrin complex interacts with the transferrin receptor (TfR) on the cell membrane, contributing to the formation of RBCs in the erythroid compartment [11]. A portion of the released iron is loaded into cellular ferritin (Ft; including Ft-H and Ft-L). In the presence of oxygen, the Ft-H facilitates the oxidation of Fe^{2+} (ferrous ion) to Fe^{3+} (ferric ion). Subsequently, the Ft-L stores this Fe^{3+} [12]. The Ft-L features a nucleation site, consisting of a cluster of cavity-exposed carboxyl residues, which readily bind to Fe^{3+}, thereby simplifying the storage process [13]. When the body's iron metabolism is vigorous, nuclear receptor coactivator 4 (NCOA4) can recognize Ft-H, bring Ft into the lysosomal pathway for degradation, and release iron in Ft for iron utilization in the body [14]. However, some iron is free in cells in the form of ferrous iron (Fe^{2+}), which is well known to be

90 an important initiator of free radical oxidation. Moreover, the accumulation of large
91 amounts of Fe^{2+} ions in cells may cause ferroptosis [15].

92 Despite the extensive study of erythropoiesis under HA/HH conditions, the precise
93 effects of HA/HH on erythrophagocytosis within the spleen remain largely
94 unexplored. Considering the significant role of the spleen in RBC processing and the
95 crucial function of RPMs in iron recycling from RBC clearance, we evaluated the
96 impacts of HA exposure on the spleen/splenic macrophages using an HH-exposed
97 mouse model (simulating 6000 m exposure conditions). In the current study, we
98 sought to further investigate whether high-altitude/hypobaric hypoxia (HA/HH) can
99 influence the erythrocyte disposal and iron recycling processes in macrophages. More
100 specifically, we aimed to determine the potential impact of HA/HH exposure on the
101 integrity of the erythrophagocytosis process. We discovered that exposure to HH
102 triggered ferroptosis in the spleen, particularly in macrophages. This led to a reduction
103 in macrophage numbers, which was subsequently followed by disruptions in eryptosis
104 and iron recycling within the spleen. These findings may hold clinical significance,
105 particularly in the context of continuous pathological erythrocytosis and the
106 progression of HAPC under HA exposure.
107

108 ## Methods

109 **HH mouse exposure model**

110 Male C57BL/6 male mice (at 8 weeks of age) were obtained from the animal
111 experimental centre of Nantong University. Mice were adapted to the facilities for 3
112 days before experiments. Mouse models of HH exposure were established by placing

113 the mice in the decompression chamber (TOW-INT TECH, ProOx-810, China) for 1 d,
114 2 d, 3 d, 7 d, and 14 d. The parameters were set as follows: 6000 m above sea level,
115 oxygen partial pressure of 11 kPa, lifting speed of 20 m/s, chamber pressure of 54 kPa,
116 temperature of 25 ℃, humidity of 40%, and 12-h light/dark cycles. Tuftsin (1.5 mg/kg,
117 MCE, HY-P0240, USA) was used to stimulate the phagocytosis of macrophages [16],
118 and was injected at 7 d and 11 d during the 14-d period of mice exposed to HH.

119 **Splenic macrophage culture and treatments**

120 After isoflurane anaesthesia, mice were transcardially perfused with precooled PBS,
121 and then splenic tissue was collected. The spleen was then dissected into minuscule
122 fragments, each approximately 1 mm^3 in volume, and separated in cold, phenol
123 red-free Hanks' balanced salt solution (HBSS; Gibco, Grand Island, NY, USA). The
124 cell extracts were centrifuged at 500 rpm for 5 min at 4 ℃. The pellets were then
125 resuspended and incubated with ammonium-chloride-potassium (ACK) lysing buffer
126 (Thermo Fisher Scientific, USA) for 3 min at room temperature. Next, cell extracts
127 were purified in a four-phase Percoll (Sigma–Aldrich, St. Louis, MO, USA) gradient:
128 0, 30, 40, and 50% in HBSS. After centrifugation at 500 rpm for 20 min at 4°C, the
129 macrophage-enriched fraction was collected at the interface between the 30% and 40%
130 phases. Cells were washed in two rounds with HBSS and then resuspended in AIM V
131 medium (Thermo Fisher Scientific). The cells in this medium were cultured at 37 ℃
132 and 5% CO_2 for 12 h. After the cells were treated with ferrostatin-1 (Fer-1, 2 μm;
133 Selleck Chemicals, S7243, USA) 1 h in advance, the cells were placed in a hypoxia
134 workstation (Invivo2, Ruskinn, UK) for 24 h.

135 **Blood smear and hematological indices**

136 The collected blood was gently mixed with EDTA (15 g/L) to obtain anticoagulant
137 blood, which was detected by a hematology analyser (XE-5000, Sysmex Corporation,
138 Japan). Blood smear preparation method: a blood sample is dropped onto a slide, and
139 another slide is used to push the blood sample into a uniform thin layer at a constant
140 speed. After the blood samples were dried, Wright's stain solution was added and
141 incubated for 1 min. Then, the slide was rinsed with water. Blood smears were
142 photographed with a DM4000B microscope (Leica, Germany).

143 **Lillie staining**

144 The Lillie staining method was employed to ascertain Fe^{2+} deposition within the
145 spleen, according to the protocol delineated by Liu et al [17]. Briefly,
146 paraffin-embedded spleen sections underwent a process of dewaxing and rehydration
147 via xylene and gradient alcohol. Then, the Lillie staining solution (G3320, Solarbio,
148 China) was applied at 37°C for 50 min in a light-restricted environment, improved by
149 a 5-min PBS wash. Subsequently, a mixture comprising 30 % hydrogen peroxide and
150 methanol was incubated for 20 min, and then the sections were subjected to two
151 5-min washes with PBS. The DAB developing solution, which is not included in the
152 Lillie bivalent iron staining kit, was applied for light-sensitive staining. The sections
153 were stained with a nuclear fast red solution in a light-restricted setting for 10 minutes,
154 followed by a 5-second wash with ddH_2O. Lastly, the sections were dehydrated with
155 gradient alcohol, cleared with xylene, and mounted with neutral resin.

156 **Wright staining**

157 Mice were anaesthetized and perfused with saline. The spleen was subsequently
158 excised to prepare a single cell suspension, achieved by filtering through a 70 μm
159 filter. Samples were centrifuged at 500 g for 5 min for cell separation. The cell pellet
160 was subjected to three PBS washes. The suspension was then smeared onto a slide
161 and air-dried. Following this, the slide was stained with Wright solution (G1040,
162 Solarbio, China) for 3 min. An equivalent volume of pH 6.4 phosphate buffer was
163 introduced, and the slide was gently agitated to allow mixing with the Wright's stain
164 solution for 5 min. After washing and drying, a microscope (DM4000B, Leica,
165 Germany) was utilized for visualization and image acquisition.

166 **Western blot**

167 Tissue and cell samples were homogenized on ice after cell lysates and protease
168 inhibitors were added. Centrifugation was performed at 12,000 rpm for 15 min at 4°C
169 to collect the supernatant. Protein concentration was determined by the BCA detection
170 method. A sample containing 30 μg protein was loaded and run in each well of SDS–
171 PAGE gels. The membranes were incubated with the following antibodies: HO-1
172 (1:2000, Abcam, ab13243, USA); Ft-L (1:1000, Abcam, ab69090, USA); Ft-H
173 (1:1000, Novus, NBP1-31944, USA); NCOA4 (1:1000, Santa Cruz, sc-373739, USA);
174 TfR (1:1000, Thermo Fisher, 13-6800, USA); Fpn (1:1000, Novus, NBP1-21502,
175 USA); ACSL4 (1:1000, Santa Cruz, sc-271800, USA); xCT (1:1000, Proteintech,
176 26864-1-AP, USA); Gpx4 (1:1000, Abcam, ab125066, USA); CD206 (1:1000, RD,
177 AF2535, USA); CD16 (1:2000, RD, AF1960, USA); and β-actin (1:1000, Sigma–
178 Aldrich, A5316, USA). The secondary antibodies were as follows: goat anti-mouse

179 (1:10000, Jackson, USA) and goat anti-rabbit (1:10000, Jackson, USA). The gray
180 value of specific blots was scanned and analysed using ImageJ software (National
181 Institute of Health, USA).
182
183 **RT–PCR analysis**
184 Total RNA extraction and RT–PCR analysis were performed essentially as described
185 previously [18]. Primer sequences were as follows:
186

Gene	Primer sequence (5'-3')	Product length (bp)
Csf1	F: GGCTTGGCTTGGGATGATTCT R: GAGGGTCTGGCAGGTACTC	126
Csf2	F: GGCCTTGGAAGCATGTAGAGG R: GGAGAACTCGTTAGAGACGACTT	104
CCL2	F: TTAAAAACCTGGATCGGAACCAA R: GCATTAGCTTCAGATTTACGGGT	121
CCL7	F: GCTGCTTTCAGCATCCAAGTG R: CCAGGGACACCGACTACTG	135

187
188 **GEO analysis**
189 GSE46480 samples were found in the GEO database of NCBI with the keyword
190 "High Altitude" search. The data set was divided into two groups, one for the plain
191 (Base Camp) and the other for the plateau (Altitude), with a sample size of 98 for
192 each group. Blood samples were collected from the same person at McMurdo Station
193 (48 m) and immediately transferred to Amundsen-Scott South Pole Station (2835 m)
194 on the third day. R language was used for data analysis, and GraphPad Prism was
195 used for statistics.
196

197 **Malondialdehyde (MDA), Cysteine (Cys) and Glutathione (GSH) content**
198 **detection**
199 MDA was detected by a Micro Malondialdehyde Assay Kit (Solarbio, BC0025,
200 China). Cys was detected by a Micro Cysteine Assay Kit (Solarbio, BC0185, China).
201 GSH was detected by a Micro Reduced Glutathione Assay Kit (Solarbio, BC1175,
202 China).
203 **Immunofluorescence**
204 Spleen sections of 9 μm thickness were flash-frozen and stored at -80°C. Before
205 immunofluorescence staining, these sections were allowed to acclimate to room
206 temperature for 30 minutes, then incubated in 10% BSA-PBS for 10 minutes. Next,
207 the sections were incubated overnight with F4/80-PE (1:200, Biolegend, 123110,
208 USA) and then washed thrice with PBS. Due to the limitations of F4/80 as a definitive
209 macrophage marker, we concurrently conducted immunohistochemical analysis for
210 heme oxygenase-1 (HO-1) (1:200, Abcam, ab13243, USA). Following this, sections
211 were washed thrice with 0.05% PBST, incubated with secondary antibodies
212 DAR-Alexa555 at room temperature for 2 hours, washed thrice with PBS again, and
213 finally sealed with 50% glycerine-PBS. Fluorescence microscopy images were
214 captured using a confocal laser scanning microscope (SP8, Leica Microsystems,
215 Wetzlar, Germany). To quantify the immunostaining intensity of F4/80 and HO-1, we
216 utilized ImageJ software. Specifically, we captured multiple fields of view for each
217 slide, and the software was used to measure the mean intensity of the fluorescent
218 signal in these images. These measurements were then normalized to the NN group to

219 account for any experimental variations.

220 **Tissue iron staining (DAB-enhanced Perls' staining)**

221 DAB-enhanced Perls' staining for the spleen paraffin sections was performed as
222 described previously [19]. Briefly, the sections were washed with PBS and cultured in
223 freshly prepared Perls' solution (1% potassium ferricyanide in 0.1 M hydrochloric
224 acid buffer). The slides were then immersed and stained with DAB. All slides were
225 counterstained with hematoxylin and visualized under a DM4000B microscope (Leica,
226 Germany). Data were collected from three fields of view per mouse and
227 semiquantitatively analysed with ImageJ software. Quantitative results of iron
228 staining were finally normalized to the NN control group.

229 **Flow cytometry**

230 1) The steps of reticulocyte ratio detection were as follows: Whole blood was
231 extracted from the mice and collected into an anticoagulant tube, which was then set
232 aside for subsequent thiazole orange (TO) staining [20]. The experimental tube and
233 negative control tube were prepared, 125 μL normal saline, 4 μL anticoagulant and
234 125 μL TO working solution (1 μg/mL, Sigma, 390062, USA) were added to each
235 tube, and 250 μL normal saline and 4 μL anticoagulant were added to each tube of the
236 negative control tube. After incubation at room temperature for 1 h, flow cytometry
237 analysis was carried out by using the FL1 (488 nm/525 nm) channel.

238 2) The steps for the determination of intracellular divalent iron content and lipid
239 peroxidation level were as follows: Splenic tissue was procured from the mice and
240 subsequently processed into a single-cell suspension using a 40 μm filter. The RBCs

241 within the entire sample were subsequently lysed and eliminated, and the remaining
242 cell suspension was resuspended in PBS in preparation for ensuing analyses. A total of
243 1×10^6 cells were incubated with 100 μL of BioTracker Far-red Labile Fe^{2+} Dye (1
244 mM, Sigma, SCT037, USA) for 1 h or C11-Bodipy 581/591 (10 μM, Thermo Fisher,
245 D3861, USA) for 30 min. After the cells were washed with PBS twice, flow
246 cytometry analysis was carried out by using the FL6 (638 nm/660 nm) channel for
247 determination of intracellular divalent iron content or the FL1 (488 nm/525 nm)
248 channel for determination of lipid peroxidation level.

249 3) The steps for detecting the mortality of spleen cells and peritoneal macrophages
250 were as follows: 1×10^6 cells were incubated at room temperature for 40 min with 2
251 μM Calcein AM and 8 μM PI. Flow cytometry analysis was carried out by using FL1
252 (488 nm/525 nm, Calcein AM) and FL3 (488 nm/620 nm, PI) channels.

253 4) The steps for detecting the number of M1/M2 macrophages in the spleen were as
254 follows: 1×10^6 cells were incubated with 2% mouse serum-PBS for 10 min,
255 incubated with F4/80-PE (1:200), CD86-PE/Cyanine7 (1:20, Biolegend, 105014,
256 USA), and CD206-Alexa 647 (1:80, BD, 565250) for 30 min, and washed with 2%
257 mouse serum-PBS twice. Flow cytometry analysis was carried out by using FL2 (488
258 nm/575 nm, F4/80- PE), FL5 (488 nm/755 nm, CD86- PE/Cyanine7) and FL6 (638
259 nm/660 nm, CD206- Alexa 647) channels.

260 5) The steps for detecting the number of monocytes in blood, spleen and bone
261 marrow were as follows: 1×10^6 cells were incubated with 2% mouse serum-PBS for
262 10 min, incubated with F4/80-PE, CD11b-PE/CY7 (1:2000, BD, 552850, USA), and

263 Ly6C-APC (1:2000, Thermo Fisher, 17-5932-82) for 30 min, and washed with 2%
264 mouse serum-PBS twice. Flow cytometry analysis was carried out by using FL2 (488
265 nm/575 nm, F4/80- PE), FL5 (488 nm/755 nm, CD11b-PE/CY7) and FL6 (638
266 nm/660 nm, Ly6C-APC) channels.

267 **Phagocytosis of *E. coli* and RBCs**

268 *E. coli* was labelled with Cy5.5 (5 mg/mL), and RBCs were labelled with NHS-biotin
269 (20 mg/mL). Macrophages (1×10^6) were coincubated with *E. coli*-Cy5.5 or
270 RBC-Biotin for 30 min and washed with 2% mouse serum-PBS twice. Flow
271 cytometry analysis was carried out by using FL6 (638 nm/660 nm) to determine the
272 phagocytosis of spleen by *E. coli*. Macrophages (coincubated with Biotin-RBCs) were
273 incubated with streptavidin-FITC for 3 h and washed twice with 2% mouse serum
274 PBS. FL1 (488 nm/525 nm) was used for flow cytometry analysis to determine the
275 phagocytosis of RBCs in the spleen.

276 **Single-cell RNA Sequencing**

277 The spleen tissues were surgically removed and stored in MACS Tissue Storage
278 Solution (Miltenyi Biotec, Bergisch Gladbach, Germany) until processing. Single-cell
279 dissociation was performed by the experimentalists at the GENECHEM laboratory
280 (Shanghai, China). Dissociated single cells were then stained for viability assessment
281 using Calcein-AM (BD Biosciences, USA) and Draq7 (BD Biosciences). The BD
282 Rhapsody system was used to capture transcriptomic information from single cells.
283 Single-cell capture was achieved by random distribution of a single-cell suspension
284 across >200,000 microwells through a limited dilution approach. Beads with

oligonucleotide barcodes were added to saturation so that a bead was paired with a cell in a microwell. The cells were lysed in the microwell to hybridize mRNA molecules to barcoded capture oligos on the beads. Beads were collected into a single tube for reverse transcription and ExoI digestion. Upon cDNA synthesis, each cDNA molecule was tagged on the 5′ end (that is, the 3′ end of an mRNA transcript) with a unique molecular identifier (UMI) and cell barcode indicating its cell of origin. Whole transcriptome libraries were prepared using the BD Rhapsody single-cell whole-transcriptome amplification (WTA) workflow, including random priming and extension (RPE), RPE amplification PCR and WTA index PCR. The libraries were quantified using a High Sensitivity D1000 ScreenTape (Agilent) and High Sensitivity D1000 Reagents (Agilent) on a 4150 TapeStation System (Agilent, Palo Alto, CA, USA) and the Qubit High Sensitivity DNA assay (Thermo Fisher Scientific). Sequencing was performed on an Illumina sequencer (Illumina Nova Seq 6000, San Diego, CA) in a 150 bp paired-end run.

Statistical analysis

Statistical analysis was conducted using GraphPad Prism 8.0 software. All values were represented as the mean ± standard error (SEM). The homogeneity of variance was verified before the application of a parametric test. A two-tailed Student's t-test was employed for data from two groups, while a one-way analysis of variance (ANOVA) with multiple comparisons using Tukey's post hoc test was utilized for data from multiple groups. A p-value of less than 0.05 was considered statistically significant.

307

308 ## Results

309 **HH exposure promotes erythrocytosis in mice**

310 To mimic 6000 m HA exposure, we placed C58BL/6 mice in an animal hypobaric
311 oxygen chamber and detected the blood indices in the blood of the mice after HH
312 exposure for different times. The blood smear showed that the number of RBCs was
313 increased from 3 to 14 days after HH exposure compared with the normobaric
314 normoxia (NN) group (Figure 1A). Routine blood tests further confirmed the results
315 in blood smears, which showed that the RBC number (Figure 1B), HGB content
316 (Figure 1C) and HCT value (Figure 1D) were all increased significantly to varying
317 degrees, while MCH was not changed after HH exposure (Figure 1E). We further
318 performed flow cytometry by TO staining to detect reticulocytes after 7 and 14 days
319 of HH treatment. The results showed that at both HH 7 and 14 d of exposure, the
320 reticulocyte proportion was increased (Figure 1F). These results suggested that the
321 HH-treated mouse model mimics HA exposure well, which promotes erythropoiesis
322 and results in erythrocytosis in mice following HH exposure.

323

324 **Spleen inhibits the immoderate increase in RBCs under HH conditions**

325 To determine the roles of the spleen in RBC homeostasis under HA/HH, we
326 investigated the effects of HH on the morphology, volume and weight of the spleen as
327 well as erythrocyte indices. As shown in Figure 2, the spleen volume and weight were
328 decreased significantly after HH exposure for 1 day compared to NN treatment

329 (Figure 2, A-C). However, the spleen was obviously enlarged from 2 to 14 days after
330 HH exposure (Figure 2, A-C). The results indicated that the spleen contracted, the
331 stored RBCs in the spleen were released into the blood at 1 day, and the RBCs were
332 produced and/or retained in the spleen from 2 to 14 days after HH exposure. In our
333 research, we also examined the influence of the spleen on RBCs homeostasis under
334 HH conditions. We investigated whether the role of spleen in RBCs clearance under
335 HH conditions could be compensated by the liver or other components of the
336 mononuclear macrophage system. To conduct this, we performed splenectomies on
337 mice and subsequently exposed them to HH conditions for 14 days. This allowed us
338 to monitor RBCs counts and blood deposition. Our findings indicated that, in
339 comparison to both the splenectomized mice under NN conditions and the
340 sham-operated mice exposed to HH, erythrocyte deposition (Figure 2D) and counts
341 (Figure 2E), as well as HGB (Figure 2F) and HCT (Figure 2G) levels, significantly
342 increased 14 days post-splenectomy under HH conditions. Meanwhile, MCH levels
343 remained stable (Figure 2H). These indices did not vary in mice, regardless of
344 whether they had undergone a splenectomy, under NN conditions (Figure 2D and E).
345 These results suggest that the liver and other mononuclear macrophages do not
346 effectively compensate under HH conditions. Furthermore, our research highlights the
347 crucial role of the spleen in maintaining RBCs homeostasis under conditions of HH.
348 The study suggests that the spleen functions to regulate the proliferation of RBCs,
349 preventing their overproduction in response to HH exposure.
350

351 **Reduction of splenic macrophages due to HH exposure**

352 Considering macrophages as the primary cell type responsible for processing RBCs
353 within the spleen under physiological conditions, we subsequently investigated the
354 population and activity of these macrophages after exposure to HH for 7 or 14 days,
355 employing flow cytometry and single-cell sequencing techniques. Calcein/PI double
356 staining, examined via flow cytometry, revealed a significant decrease in viable
357 spleen cells and a concurrent increase in dead cells following 7 and 14 days of HH
358 exposure (Figure 3, A-C). Single-cell sequencing further disclosed a significant
359 reduction in splenic macrophages after 7 days of HH exposure (Figure 3, D-F).
360 Additionally, the expressions of CD16 (M1 macrophage marker) and CD206 (M2
361 macrophage marker) were observed to decrease after both 7 and 14 days of HH
362 exposure (Figure 3, G-L). Western blot analysis corroborated the flow cytometry
363 findings, showing a decrease in mature macrophages ($F4/80^+/CD11b^+$), including both
364 M1-type ($F4/80^+/CD86^+$) and M2-type ($F4/80^+/CD206^+$) macrophages, in the spleens
365 of mice after 7 days of HH exposure (Figure 3M). To further elucidate the migration
366 and differentiation of monocytes from the bone marrow to the spleen, we analyzed the
367 expression of chemokines CCL2, CCL7, Csf1, and Csf2 in the spleen using qPCR and
368 determined the number of monocytes in the bone marrow (BM) and spleen via flow
369 cytometry. Our results indicated a significant reduction in the expression of CCL2,
370 CCL7 (Figure 3N), Csf1, and Csf2 (Figure 3O) in the spleen after 7 and 14 days of
371 HH exposure. Furthermore, the number of monocytes ($Ly6C^+/CD11b^+$) in the bone
372 marrow (Figure 3, P-R) and spleen (Figure 3, P and S-T) also exhibited a decline after

373 7 and 14 days of HH exposure. We evaluated the depletion of macrophages in the
374 spleen under HH conditions by examining the expression and distribution of HO-1
375 and F4/80. Figures 3U-W depict a decrease in both HO-1 and F4/80, predominantly
376 within the spleen's red pulp following HH exposure. Together, these findings indicate
377 a reduction in the number of splenic macrophages after HH exposure, which could
378 impair the spleen's capacity to process erythrocytes.
379
380 **The impact of HH exposure on erythrophagocytosis and iron processing capacity**
381 **of the spleen**
382 We investigated the influence of HH exposure on erythrocyte phagocytosis and heme
383 iron recycling within splenic macrophages. We administered NHS-biotin
384 intravenously to the mice followed by HH treatment in vivo. The clearance of RBCs
385 was monitored by detecting the retention of biotin-labelled RBCs using flow
386 cytometry in both the blood and spleen of the HH-treated mice. We observed a
387 substantial decrease in biotin-labelled RBCs in the blood and spleen cells at 7- and
388 14-days post HH exposure (Figure 4, A-D). Despite the natural decrease of labelled
389 RBC over time, the decay was more pronounced in the HH exposure group compared
390 to the normobaric normoxia (NN) group in both the blood (Figure 4, A and C) and
391 spleen (Figure 4, B and D). The phagocytic ability of mouse spleen macrophages
392 towards RBCs was significantly more impaired after HH exposure, particularly on the
393 14th day (Figure 4, A-D). Additionally, to substantiate our findings, we quantified the
394 retention of RBC counts by Wright staining in splenic cells after 7 and 14 days of HH

395 exposure (Figure 4, E-F). This confirmed impaired erythrophagocytosis in the spleen
396 under HH exposure, as evidenced by an increase in deformation and retention of
397 RBCs following 7 and 14 days of HH exposure. Furthermore, we employed Tuftsin to
398 stimulate phagocytosis of macrophages and carried out immunofluorescence and iron
399 staining to examine the heme iron recycling capability of the spleen under HH
400 conditions (Figure 4G). As depicted in Figure 4H, compared with the NN group,
401 F4/80 expression and iron deposition in the red pulp were significantly reduced after
402 HH exposure. However, Tuftsin led to an induction of F4/80 expression and iron
403 deposition in the red pulp of the spleen under HH (Figure 4, I-L). These results imply
404 that the capacity for erythrocyte phagocytosis and heme iron recycling by the spleen
405 was compromised, principally due to the reduction in macrophages in the red pulp
406 under HH conditions.
407
408 **HH exposure induces iron mobilization and ferroptosis in the spleen**
409 To elucidate the precise mechanisms underlying the macrophage reduction caused by
410 HH, we examined the expression of proteins related to iron metabolism and
411 ferroptosis in mice treated with HH and analyzed the corresponding gene expression
412 in peripheral blood mononuclear cells (PBMCs) from healthy humans acutely
413 exposed to HA conditions using GEO data (No. GSE46480). The results showed that,
414 compared to the NN group, the expression levels of HO-1, Ft-L, Ft-H, NCOA4, and
415 xCT were decreased, while Fpn, TfR, and ACSL4 expressions were significantly
416 increased after 7 and 14 days of HH exposure (Figure 5, A-B, D-E; Figure S1, A-D).

417 With the exception of NCOA4, the alterations in gene expressions related to iron
418 metabolism and ferroptosis in PBMCs were consistent with our Western blot results
419 (Figure 5, C and F). The GPX4 gene and protein expressions remained largely
420 unchanged in both human PBMCs and mouse spleens. The changes in iron
421 metabolism- and ferroptosis-related genes in PBMCs reflect the protein changes in the
422 spleen under HH exposure. We detected Fe^{2+} and lipid ROS levels in the spleen by
423 flow cytometry, and quantified MDA, GSH, and Cys levels using biochemical
424 detection kits. As depicted in Figure 5, G and H; Figure S1, I-K, the Fe^{2+} (Figure 5G;
425 Figure S1, E and F) and lipid ROS (Figure 5H; Figure S1, G and H) levels in the
426 spleen increased significantly after HH exposure. Additionally, the MDA content
427 (Figure 5I; Figure S1I) in the spleen increased, whereas Cys (Figure 5J; Figure S1J)
428 and GSH (Figure 5K; Figure S1K) levels significantly decreased after HH exposure.
429 To ascertain the increased Fe^{2+} primarily emanated from the red pulp, we detected
430 Fe^{2+} deposition and distribution in the spleen by Lillie stain following 7 and 14 days
431 of HH exposure (Figure 5, L-M; Figure S1, L-M). These results demonstrated
432 increased Fe^{2+} primarily deposited in the red pulp of the spleen. Taken together, these
433 findings suggest that iron mobilization in the spleen was enhanced and ferroptosis was
434 induced after 7 days of HH exposure.
435
436 **Hypoxia induces ferroptosis in primary splenic macrophages**
437 To investigate whether hypoxia exposure can trigger ferroptosis in macrophages, we
438 measured alterations in Fe^{2+} and lipid ROS levels, cell viability, phagocytosis, and

439 ferroptosis-related protein expressions in primary splenic macrophages under hypoxia
440 in the presence of a ferroptosis inhibitor (Fer-1). As depicted in Figure 6, compared
441 with the normoxia control group (Nor), Fe^{2+} (Figure 6, A-C) and lipid ROS (Figure 6,
442 D-E) levels significantly increased, whereas the number of viable cells (Figure 6G-H)
443 and phagocytosis ability (Figure 6I) significantly decreased after 24 h of hypoxia
444 (Hyp) treatment. In addition, prolonged hypoxia exposure led to a gradual increase in
445 ACSL4 expression, while xCT and GPX4 expressions decreased (Figure 6F). Fer-1
446 mitigated the increase in Fe^{2+} content (Figure 6, J-K) and reversed the expression
447 changes in ACSL4, xCT, and GPX4 induced by hypoxia exposure (Figure 6, L-O).
448 Simultaneously, Fer-1 reversed the alterations in MDA, Cys, and GSH levels induced
449 by hypoxia (Figure 6, P-R). These findings confirm that hypoxia induced ferroptosis
450 in primary splenic macrophages.
451

452 **Discussion**

453 The purpose of this study was to explore the effects and mechanisms of HA/HH
454 exposure on erythrophagocytosis and iron circulation in mouse spleens. Here, we used
455 an HH chamber to simulate 6000 m HA exposure and found that HH exposure
456 induced iron mobilization and activated ferroptosis in the spleen, especially in red
457 pulp macrophages (RPMs), which subsequently inhibited the phagocytosis and
458 clearance of RBCs. Finally, chronic exposure to HA/HH may promote the retention of
459 RBCs in the spleen, cause splenomegaly, advance RBC production, and promote the
460 occurrence and development of HAPC (Figure 7).

461 RBCs/erythrocytes are the carriers of oxygen and the most abundant cell type in the
462 body. Erythrocytes are rapidly increased by triggering splenic contraction in acute
463 HA/HH exposure [21] and stimulating erythropoiesis in subsequent continuous or
464 chronic HA/HH exposure. Changes in spleen morphology and size are closely related
465 to the spleen's ability to recover RBCs [22], and studies have shown that the spleen is
466 in a contraction state after short-term exposure to HA/HH, and approximately 40% of
467 the increase in RBCs is due to the contraction of the spleen [21, 23, 24]. In the present
468 study, mice were treated under HH to mimic HA exposure (mainly mimicking the low
469 oxygen partial pressure environment of 6000 m HA) for different times according to
470 other studies [25, 26]. Our results showed that HH exposure not only significantly
471 increased the RBC and HGB contents but also significantly increased $CD47^+$ cells in
472 blood. However, short-term (1 d) HH exposure caused spleen contraction and induced
473 splenomegaly after 3 d of HH treatment. This contraction can trigger an immediate
474 release of RBCs into the bloodstream in instances of substantial blood loss or
475 significant reduction of RBCs. Moreover, elevated oxygen consumption rates in
476 certain animal species can be partially attributed to splenic contractions, which
477 augment hematocrit levels and the overall volume of circulating blood, thereby
478 enhancing venous return and oxygen delivery [27, 28]. Thus, we hypothesized that the
479 body, under such conditions, is incapable of generating sufficient RBCs promptly
480 enough to facilitate enhanced oxygen delivery. Consequently, the spleen reacts by
481 releasing its stored RBCs through splenic constriction, leading to a measurable
482 reduction in spleen size. These results are consistent with other research results; that is,

483 HH or HA exposure affects spleen morphology and further affects RBC counts and
484 HGB levels [29-31]. Considering these findings, the present study postulates that
485 hypoxia-induced inhibition of erythrophagocytosis may lead to RBC retention.
486 However, we acknowledge that the manuscript in its current preprint form does not
487 offer conclusive evidence to substantiate this hypothesis. To bridge this gap, we
488 further conducted experiments where the spleen was perfused, and total cells were
489 collected post HH exposure. These cells were then smeared onto slides and subjected
490 to Wright staining. Our results unequivocally demonstrate an evident increase in
491 deformation and retention of RBCs in the spleen following 7 and 14 days of HH
492 exposure. This finding strengthens our initial hypothesis and contributes a novel
493 perspective to the understanding of splenic responses under hypoxic conditions.

494 HAPC is a common chronic HA disease characterized by excessive proliferation of
495 RBCs caused by HH conditions [32]. Under physiological conditions, RBC
496 homeostasis is maintained by balancing erythropoiesis and erythrocyte clearance [4].
497 The ability of RBC disposal in the spleen for iron recycling under HA/HH exposure
498 was important to RBC regeneration in bone marrow (BM) [33]. Thus, we
499 hypothesized that erythrophagocytosis and iron recycling in the spleen were altered
500 by HA/HH exposure and further disturbed RBC homeostasis and affected the
501 progression of HAPC. We found that compared with sham group mice, HH
502 significantly increased the contents of RBCs and HGB in the blood of splenectomy
503 mice. This strongly verified that the spleen is a key organism that maintains RBC
504 magnitude within a certain range of physiological statuses under HA/HH conditions.

505 As originally proposed by Metchnikoff in the 19th century, macrophages,
506 especially RPMs, play a pivotal role in the regulation of RBCs and iron homeostasis
507 [34, 35]. We detected the macrophage population in the spleen and found that HH
508 exposure for 7 and 14 days reduced the total macrophage and M1- and M2-type
509 macrophage proportions in the spleen. This result is supported by another study, that
510 is, hypoxia reduces M1-type macrophages in human gastric cancer [36]. We next
511 observed whether monocyte migration and differentiation from the BM to the spleen
512 replenish reduced macrophages and sustain macrophage homeostasis after HH
513 treatment. It is well known that splenic erythropoiesis is a dynamic process [4]. Upon
514 phagocytosing erythrocytes in macrophages, spleen tissue (including macrophages
515 and fibroblasts) produces the chemokine C–C motif chemokine ligand 2 and 7 (CCL2
516 and CCL7) to recruit blood monocytes to the spleen [37, 38]. Unlike most studies in
517 tumours, which mainly suggested that macrophage accumulation in hypoxic areas was
518 derived by enhanced chemokine expression in tumours [39, 40], CCL2, CCL7 and
519 Csf1 expression was decreased in the spleen after HH exposure for 7 and 14 days in
520 our study. Furthermore, we found that HH exposure inhibited Ly6C^{hi} monocyte
521 migration from the BM to spleen, where these cells subsequently differentiated into
522 RPMs. The combination of decreased splenic RPMs, along with the reduced
523 BM-derived Ly6C^{hi} monocytes, suggests that the homeostasis of the RPM population
524 of circulating monocytes was also inhibited after the RPM depletion induced by HH
525 exposure. The observed decrease in monocytes within the BM is likely attributable to
526 the fact that monocytes and precursor cells for RBCs both originate from the same

527 hematopoietic stem cells within the BM [41]. As such, the differentiation to monocyte
528 is reduced under hypoxic conditions, which may subsequently cause a decrease in
529 migration to spleen. Furthermore, we hypothesize that an increased migration of
530 monocytes to other tissues under HH exposure may also contribute to the decreased
531 migration to the spleen. The liver, which partially contributes to the clearance of
532 RBCs, may play a role in this process. Our investigations to date have indeed
533 identified an increased monocyte migration to the liver. We were pleased to discover
534 an elevation in CSF1 expression in the liver following HH exposure for both 7 and 14
535 days. This finding was corroborated through flow cytometry, which confirmed an
536 increase in monocyte migration to the liver.

537 HO-1 is a major antioxidant and cytoprotective enzyme that catalyzes the
538 degradation of heme to provide heme homeostasis and protect against free
539 heme-induced toxicity [42]. In addition, it was supposed that mice deficient in HO-1
540 are largely devoid of RPMs and suggested that HO-1 is critical for RPM development
541 and survival after erythrocyte clearance [43]. The reduced HO-1 protein of red pulp in
542 our study also implied decreased macrophage accounts induced by HH exposure,
543 although HO-1 was considered to be upregulated by hypoxia-inducible factor 1
544 (HIF-1) under hypoxia [44, 45]. Along with the decreased macrophage amount
545 induced by HH, the phagocytic ability of macrophages in the spleen was also
546 inhibited both *in vitro* and *in vivo*. Meanwhile, the injection of tufftsin strongly
547 confirmed the enhancement of heme iron processing in the spleen under HH exposure.
548 Nevertheless, our data conflict with the study of Anand *et al*, which reported that

549 hypoxia causes an increase in phagocytosis by macrophages in a HIF-1α-dependent
550 manner [46]. This may be because they performed intermittent hypoxia, while we
551 used consistent hypoxia in the present study.

552 Macrophages play a crucial role in maintaining erythrocyte homeostasis, partially
553 due to their function in digesting the HGB content of cleared RBCs and recycling the
554 iron back to erythroid progenitors for heme synthesis and HGB production [47]. In
555 mammals, the majority of bodily iron exists in the form of heme, with the most
556 substantial pool comprising HGB [48]. HGB contains four prosthetic hemoglobins,
557 and each mature RBC is thought to contain approximately 1.2×10^9 heme moieties
558 [47]. As previously mentioned, the majority of iron required to sustain erythropoiesis
559 is derived from recycled RBCs. In general, RPMs are equipped with molecular
560 machinery capable of neutralizing the toxic effects of heme and metabolizing iron [49,
561 50]. Nonetheless, any disruptions in the process of erythrophagocytosis, the uptake
562 and degradation of erythrocytes by macrophages, could potentially result in abnormal
563 iron metabolism, potentially manifesting as conditions such as anemia or iron
564 overload [49]. The release of heme upon processed RBCs constitutes a permanent and
565 considerable threat for iron cytotoxicity in macrophages and may eventually result in
566 a specific form of programmed cell death termed ferroptosis [51], which may cause
567 decreased cell counts [52, 53].

568 Accordingly, we investigated the iron metabolism status and explored ferroptosis in
569 spleen/macrophages after HH/hypoxia treatment and found that HH exposure
570 prompted iron mobilization, especially in ferritinophagy and lipid peroxidation in the

spleen. Interestingly, we found that except for NCOA4, all the gene expression changes in the PBMCs of humans after acute HA exposure were similar to the changes in the spleens of mice after HH exposure for 7 and 14 days. This is probably because NCOA4 in the spleen mediates iron release from Ft-L and facilitates iron reuse, while PBMCs do not possess this function *in vivo*. These results not only indicated that HH exposure induces spleen ferroptosis but also implied that the gene expression changes in PBMCs under HA/HH may reflect RBC processing functions in the spleen and further indicate the iron metabolism status in the clinic. We further found that the exact mechanism of macrophage ferroptosis induced by HH exposure was caused by increased Fe^{2+} and decreased antioxidative system expression, which finally resulted in lipid peroxidation of macrophages. It has been proposed that heme catabolism by HO-1 protects macrophages from oxidative stress [49]. The enhanced ROS and lipid peroxidation *in vivo* were also consistent with the decreased HO-1 expression in the spleen. In addition, 1% hypoxia treatment induced ferroptosis *in vitro*, which was reduced by treatment with ferrostatin-1, a ferroptosis inhibitor. However, our data were inconsistent with the study of Fuhrmann *et al*., which reported that hypoxia inhibits ferritinophagy and protects against ferroptosis [54]. We hypothesized that the enhanced iron demand for new RBC regeneration in BM caused by HH leads to an increase in NCOA4 and Ft-L protein expression in the spleen. On the other hand, hypoxia inhibited anti-ferroptosis system expression, including reduced Gpx4 expression and increased lipid ROS production. The results were supported by the group of Youssef LA *et al*, who reported that increased

593 erythrophagocytosis induces ferroptosis in RPMs in a mouse model of transfusion
594 [55]. However, as most studies have reported, ferroptosis is not only characterized by
595 increased lipid ROS but also significantly shrinking mitochondria [56]. We never
596 found shrinking mitochondria in RPMs after HH exposure (data not shown). Gao *et al*.
597 proposed that mitochondria played a crucial role in cysteine deprivation-induced
598 ferroptosis but not in that induced by inhibiting glutathione peroxidase-4 (GPX4), the
599 most downstream component of the ferroptosis pathway [57]. Interestingly, in our *in*
600 *vivo* study, Gpx4 expression was also not changed after HH exposure. It is still not
601 clear whether mitochondria are involved in ferroptosis. Whether HH treatment caused
602 mitochondrial swelling directly and the exact mechanism involved in this process still
603 need to be further investigated.

604 When the splenic macrophages' phagocytic function is compromised, the burden of
605 managing the increased number of RBCs falls to the other cells within the spleen, as
606 well as other clearance mechanisms within the body [58]. The endothelium, for
607 instance, has been shown to be involved in the removal of aged and damaged RBCs
608 [59]. The sinusoidal endothelial cells can recognize these RBCs, which often have
609 altered surface properties, leading to their removal from circulation [59, 60].
610 Therefore, under HH conditions, endothelial cells may play a compensatory role in
611 RBC clearance when macrophage function is impaired. Other macrophages, such as
612 liver Kupffer cells and bone marrow macrophages, may also contribute to managing
613 this buildup of RBCs [61]. Kupffer cells are the resident macrophages of the liver and
614 have significant phagocytic ability. Similarly, macrophages in the bone marrow play a

615 crucial role in iron recycling from aged erythrocytes [61, 62]. Therefore, these
616 macrophages could potentially compensate for the reduction in splenic
617 erythrophagocytosis, although their ability to effectively handle a large surge in RBC
618 numbers remains to be determined.

619 It is also possible that the spleen may adapt to the increased load of RBCs by
620 expanding the red pulp, leading to splenomegaly [63]. The red pulp is highly vascular
621 and contains numerous sinuses lined with macrophages [64]. This expansion could
622 potentially accommodate a greater number of RBCs, thus enhancing the spleen's
623 capacity for erythrophagocytosis and iron recycling. However, these compensatory
624 mechanisms may be insufficient or become overwhelmed over time, leading to
625 pathological conditions such as HAPC. Further research is necessary to fully
626 understand the consequences of splenic ferroptosis on RBC homeostasis and how
627 these effects could be mitigated or reversed. Finally, as these observations are based
628 on experimental models, they should be corroborated in human studies to assess their
629 clinical relevance and potential implications for managing conditions related to high
630 altitude exposure. The potential for therapeutic interventions that target ferroptosis,
631 erythrophagocytosis, and iron recycling should also be explored, as these could
632 provide new avenues for treating HAPC and other conditions related to high altitude
633 exposure.

634 Based on the above experiments, we first put forward the "spleen theory" of HAPC
635 (Figure 7). It hypothesizes that HH exposure induced spleen ferroptosis, especially
636 RPMs, which further inhibited erythrophagocytosis, RBC clearance, HGB processing

637 and iron recycling. This theory identifies a novel pathophysiological process in which
638 HH exposure leads to the induction of spleen ferroptosis, particularly in red pulp. As a
639 result, erythrophagocytosis, RBCs clearance, and iron recycling are impeded, causing
640 a buildup of RBCs within the spleen, leading to splenomegaly and continued RBC
641 production. The "spleen theory" of HAPC provides an intriguing new perspective on
642 the physiological responses to hypoxia and highlights the role of the spleen as a vital
643 organ in managing erythrocyte homeostasis under high altitude/hypoxic conditions.
644 These findings may be clinically relevant to the pathological conditions of HAPC
645 progression.
646

647 **Abbreviations**

648 BM: bone marrow; Cys: Cysteine; GSH: Glutathione; Ft-L: Ferritin light chains; Fpn:
649 Ferroportin; Ft: Ferritin; HH: Hypobaric hypoxia; HA: High-altitude; HAPC:
650 High-altitude polycythemia; HO-1: Heme oxygenase-1; HCT: Haematocrit; HGB:
651 Haemoglobin; HIF-1a: Hypoxia inducible factor 1 a; MCH: Mean corpuscular
652 haemoglobin; MDA: Malondialdehyde; NN: Normobaric normoxia; NCOA4: nuclear
653 receptor coactivator 4; PBMCs: peripheral blood mononuclear cells; RBC: Red blood
654 cell; RPM: Red pulp macrophage; TfR1: Transferrin receptor 1; Tf: Transferrin; TfR:
655 Transferrin receptor.
656

657 **Author contributions**

658 QQL and GHW conceived, organized, and designed the study. YQG supervised the

work. WPY, MQL, JD and JYL performed the experiments. WPY, GW and BL contributed to the analysis of data. QQL and GHW prepared, wrote and revised the manuscript. All authors contributed to read, and approved the submitted version.

Funding

This work was supported by Natural Science Foundation of China (Grants 32271228, 82171190, and 81873924), Open Cooperation Program from Key Laboratory of Extreme Environmental Medicine, Ministry of Education (KL2019GY011), China Postdoctoral Science Foundation (2020M673649), Cultivate Candidate of the Jiangsu Province "333" Project, and Nantong Municipal Science and Technology Project (MS12021020 and MS22021010).

Availability of data and materials

The datasets used and/or analyzed during the current study are available from the corresponding author on reasonable request.

Declarations

Ethics approval and consent to participate

All animal care and experimental protocols were carried out according to the Chinese Animal Management Rules of the Ministry of Health and were authorized by the Animal Ethics Committees of Nantong University research program protocol #S20190219-011. The results of the study are presented clearly, honestly, and without

681 fabrication, falsification, or inappropriate data manipulation.

682

683 **Consent for publication**

684 Not applicable.

685

686 **Competing interests**

687 The authors have no relevant financial or non-financial interests to disclose.

688

689

690 **Author details**

691 [1]Department of Physiology and Hypoxic Biomedicine, Institute of Special
692 Environmental Medicine and Co-innovation Center of Neuroregeneration, Nantong
693 University, 9 Seyuan Road, Chongchuan District, Nantong, Jiangsu 226019, China.
694 [2]College of High-Altitude Military Medicine, Institute of Medicine and Hygienic
695 Equipment for High Altitude Region, Army Medical University, Chongqing 400038,
696 China. [3]Key Laboratory of Extreme Environmental Medicine and High-Altitude
697 Medicine, Ministry of Education of China, Chongqing 400038, China. [4]Department of
698 Neurosurgery, Southwest Hospital, Army Medical University, Chongqing, Chongqing
699 400038, China.

700

References

1. Pérez-Padilla R. Impact of moderate altitude on lung diseases and risk of high altitude illnesses. Revista de investigacion clinica; organo del Hospital de Enfermedades de la Nutricion. 2022;74(5):232-43.
2. Liu X, Zhang H, Yan J, Li X, Li J, Hu J, et al. Deciphering the Efficacy and Mechanism of Astragalus membranaceus on High Altitude Polycythemia by Integrating Network Pharmacology and In Vivo Experiments. Nutrients. 2022;14(23).
3. Tymko MM, Lawley JS, Ainslie PN, Hansen AB, Hofstaetter F, Rainer S, et al. Global Reach 2018 Heightened α-Adrenergic Signaling Impairs Endothelial Function During Chronic Exposure to Hypobaric Hypoxia. Circulation research. 2020;127(2):e1-e13.
4. Dzierzak E, Philipsen S. Erythropoiesis: development and differentiation. Cold Spring Harb Perspect Med. 2013;3(4):a011601.
5. Robach P, Hansen J, Pichon A, Meinild Lundby AK, Dandanell S, Slettaløkken Falch G, et al. Hypobaric live high-train low does not improve aerobic performance more than live low-train low in cross-country skiers. Scandinavian journal of medicine & science in sports. 2018;28(6):1636-52.
6. Qiang Y, Sissoko A, Liu ZL, Dong T, Zheng F, Kong F, et al. Microfluidic study of retention and elimination of abnormal red blood cells by human spleen with implications for sickle cell disease. Proc Natl Acad Sci U S A. 2023;120(6):e2217607120.
7. Wirth F, Lubosch A, Hamelmann S, Nakchbandi IA. Fibronectin and Its Receptors in Hematopoiesis. Cells. 2020;9(12).
8. Slusarczyk P, Mandal PK, Zurawska G, Niklewicz M, Chouhan K, Mahadeva R, et al. Impaired iron recycling from erythrocytes is an early hallmark of aging. eLife. 2023;12.
9. Vahedi A, Bigdelou P, Farnoud AM. Quantitative analysis of red blood cell membrane phospholipids and modulation of cell-macrophage interactions using cyclodextrins. Scientific reports. 2020;10(1):15111.
10. Nemeth E, Ganz T. Hepcidin-Ferroportin Interaction Controls Systemic Iron Homeostasis. Int J Mol Sci. 2021;22(12).
11. Hidalgo D, Bejder J, Pop R, Gellatly K, Hwang Y, Maxwell Scalf S, et al. EpoR stimulates rapid cycling and larger red cells during mouse and human erythropoiesis. Nat Commun. 2021;12(1):7334.
12. Wang W, Grier DD, Woo J, Ward M, Sui G, Torti SV, et al. Ferritin H is a novel marker of early erythroid precursors and macrophages. Histopathology. 2013;62(6):931-40.
13. Finazzi D, Arosio P. Biology of ferritin in mammals: an update on iron storage, oxidative damage and neurodegeneration. Archives of toxicology. 2014;88(10):1787-802.
14. Bellelli R, Federico G, Matte' A, Colecchia D, Iolascon A, Chiariello M, et al. NCOA4 Deficiency Impairs Systemic Iron Homeostasis. Cell Reports. 2016;14(3):411-21.

15. von Krusenstiern AN, Robson RN, Qian N, Qiu B, Hu F, Reznik E, et al. Identification of essential sites of lipid peroxidation in ferroptosis. Nature chemical biology. 2023.
16. Corazza GR, Zoli G, Di Sabatino A, Ciccocioppo R, Gasbarrini G. A reassessment of splenic hypofunction in celiac disease. The American journal of gastroenterology. 1999;94(2):391-7.
17. Liu Z, Lv X, Yang B, Qin Q, Song E, Song Y. Tetrachlorobenzoquinone exposure triggers ferroptosis contributing to its neurotoxicity. Chemosphere. 2021;264(Pt 1):128413.
18. Luo Q, Hu J, Yang G, Yuan X, Chen Z, Wang D, et al. Fasting Increases Iron Export by Modulating Ferroportin 1 Expression Through the Ghrelin/GHSR1alpha/MAPK Pathway in the Liver. Biol Trace Elem Res. 2021;199(1):267-77.
19. Jiang H, Zhang X, Yang W, Li M, Wang G, Luo Q. Ferrostatin-1 Ameliorates Liver Dysfunction via Reducing Iron in Thioacetamide-induced Acute Liver Injury in Mice. Frontiers in pharmacology. 2022;13:869794.
20. Nébor D, Graber JH, Ciciotte SL, Robledo RF, Papoin J, Hartman E, et al. Mutant KLF1 in Adult Anemic Nan Mice Leads to Profound Transcriptome Changes and Disordered Erythropoiesis. Scientific reports. 2018;8(1):12793.
21. Schagatay E, Lunde A, Nilsson S, Palm O, Lodin-Sundstrom A. Spleen contraction elevates hemoglobin concentration at high altitude during rest and exercise. Eur J Appl Physiol. 2020;120(12):2693-704.
22. Khairullah S, Jackson N. Markers of ineffective erythropoiesis in non-transfusion dependent β-thalassaemia. Med J Malaysia. 2021;76(1):41-5.
23. Alafi MH, Cook SF. Role of the spleen in acclimatization to hypoxia. Am J Physiol. 1956;186(2):369-72.
24. Richardson M, Lodin A, Reimers J, Schagatay E. Short-term effects of normobaric hypoxia on the human spleen. European journal of applied physiology. 2008;104(2):395-9.
25. Lin HJ, Wang CT, Niu KC, Gao C, Li Z, Lin MT, et al. Hypobaric hypoxia preconditioning attenuates acute lung injury during high-altitude exposure in rats via up-regulating heat-shock protein 70. Clin Sci (Lond). 2011;121(5):223-31.
26. Brent MB, Emmanuel T, Simonsen U, Bruel A, Thomsen JS. Hypobaric hypoxia deteriorates bone mass and strength in mice. Bone. 2022;154:116203.
27. Dane DM, Hsia CC, Wu EY, Hogg RT, Hogg DC, Estrera AS, et al. Splenectomy impairs diffusive oxygen transport in the lung of dogs. Journal of applied physiology (Bethesda, Md : 1985). 2006;101(1):289-97.
28. Longhurst JC, Musch TI, Ordway GA. O2 consumption during exercise in dogs--roles of splenic contraction and alpha-adrenergic vasoconstriction. Am J Physiol. 1986;251(3 Pt 2):H502-9.
29. Holmstrom PK, Bird JD, Thrall SF, Kalker A, Herrington BA, Soriano JE, et al. The effects of high altitude ascent on splenic contraction and the diving response during voluntary apnoea. Exp Physiol. 2021;106(1):160-74.
30. Holmstrom P, Mulder E, Starfelt V, Lodin-Sundstrom A, Schagatay E. Spleen Size and Function in Sherpa Living High, Sherpa Living Low and Nepalese Lowlanders.

Front Physiol. 2020;11:647.
31. Pernett F, Schagatay F, Vildevi C, Schagatay E. Spleen Contraction During Sudden Eupneic Hypoxia Elevates Hemoglobin Concentration. Front Physiol. 2021;12:729123.
32. Wang Z, Tenzing N, Xu Q, Liu H, Ye Y, Wen Y, et al. Apoptosis is one cause of thrombocytopenia in patients with high-altitude polycythemia. Platelets. 2023;34(1):2157381.
33. Pivkin IV, Peng Z, Karniadakis GE, Buffet PA, Dao M, Suresh S. Biomechanics of red blood cells in human spleen and consequences for physiology and disease. Proc Natl Acad Sci U S A. 2016;113(28):7804-9.
34. Wynn TA, Chawla A, Pollard JW. Macrophage biology in development, homeostasis and disease. Nature. 2013;496(7446):445-55.
35. Gammella E, Buratti P, Cairo G, Recalcati S. Macrophages: central regulators of iron balance. Metallomics. 2014;6(8):1336-45.
36. Zhihua Y, Yulin T, Yibo W, Wei D, Yin C, Jiahao X, et al. Hypoxia decreases macrophage glycolysis and M1 percentage by targeting microRNA-30c and mTOR in human gastric cancer. Cancer Sci. 2019;110(8):2368-77.
37. Zhang L, Patel S, Soulakova JN, Caldwell CC, St Pierre Schneider B. Mild hypobaric hypoxia influences splenic proliferation during the later phase of stress erythropoiesis. Exp Biol Med (Maywood). 2022;247(6):509-18.
38. Bellomo A, Mondor I, Spinelli L, Lagueyrie M, Stewart BJ, Brouilly N, et al. Reticular Fibroblasts Expressing the Transcription Factor WT1 Define a Stromal Niche that Maintains and Replenishes Splenic Red Pulp Macrophages. Immunity. 2020;53(1):127-42 e7.
39. Lewis C, Murdoch C. Macrophage responses to hypoxia: implications for tumor progression and anti-cancer therapies. Am J Pathol. 2005;167(3):627-35.
40. Henze AT, Mazzone M. The impact of hypoxia on tumor-associated macrophages. J Clin Invest. 2016;126(10):3672-9.
41. Bapat A, Schippel N, Shi X, Jasbi P, Gu H, Kala M, et al. Hypoxia promotes erythroid differentiation through the development of progenitors and proerythroblasts. Experimental hematology. 2021;97:32-46.e35.
42. Vijayan V, Wagener F, Immenschuh S. The macrophage heme-heme oxygenase-1 system and its role in inflammation. Biochem Pharmacol. 2018;153:159-67.
43. Kovtunovych G, Eckhaus MA, Ghosh MC, Ollivierre-Wilson H, Rouault TA. Dysfunction of the heme recycling system in heme oxygenase 1-deficient mice: effects on macrophage viability and tissue iron distribution. Blood. 2010;116(26):6054-62.
44. Lee PJ, Jiang BH, Chin BY, Iyer NV, Alam J, Semenza GL, et al. Hypoxia-inducible factor-1 mediates transcriptional activation of the heme oxygenase-1 gene in response to hypoxia. J Biol Chem. 1997;272(9):5375-81.
45. Dawn B, Bolli R. HO-1 induction by HIF-1: a new mechanism for delayed cardioprotection? Am J Physiol Heart Circ Physiol. 2005;289(2):H522-4.
46. Anand RJ, Gribar SC, Li J, Kohler JW, Branca MF, Dubowski T, et al. Hypoxia causes an increase in phagocytosis by macrophages in a HIF-1alpha-dependent

832 manner. J Leukoc Biol. 2007;82(5):1257-65.
833 47. Korolnek T, Hamza I. Macrophages and iron trafficking at the birth and death of red
834 cells. Blood. 2015;125(19):2893-7.
835 48. Hamza I, Dailey HA. One ring to rule them all: Trafficking of heme and heme
836 synthesis intermediates in the metazoans. Bba-Mol Cell Res. 2012;1823(9):1617-32.
837 49. Soares MP, Hamza I. Macrophages and Iron Metabolism. Immunity.
838 2016;44(3):492-504.
839 50. Ganz T. Macrophages and Iron Metabolism. Microbiol Spectr. 2016;4(5).
840 51. Dixon SJ, Lemberg KM, Lamprecht MR, Skouta R, Zaitsev EM, Gleason CE, et al.
841 Ferroptosis: An Iron-Dependent Form of Nonapoptotic Cell Death. Cell.
842 2012;149(5):1060-72.
843 52. Zhang P, Chen L, Zhao QQ, Du XX, Bi MX, Li Y, et al. Ferroptosis was more initial
844 in cell death caused by iron overload and its underlying mechanism in Parkinson's
845 disease. Free Radical Bio Med. 2020;152:227-34.
846 53. Chen X, Yu CH, Kang R, Tang DL. Iron Metabolism in Ferroptosis. Front Cell Dev
847 Biol. 2020;8.
848 54. Fuhrmann DC, Mondorf A, Beifuss J, Jung M, Brune B. Hypoxia inhibits
849 ferritinophagy, increases mitochondrial ferritin, and protects from ferroptosis. Redox
850 Biol. 2020;36:101670.
851 55. Youssef LA, Rebbaa A, Pampou S, Weisberg SP, Stockwell BR, Hod EA, et al.
852 Increased erythrophagocytosis induces ferroptosis in red pulp macrophages in a
853 mouse model of transfusion. Blood. 2018;131(23):2581-93.
854 56. Xie Y, Hou W, Song X, Yu Y, Huang J, Sun X, et al. Ferroptosis: process and function.
855 Cell Death Differ. 2016;23(3):369-79.
856 57. Gao M, Yi J, Zhu J, Minikes AM, Monian P, Thompson CB, et al. Role of
857 Mitochondria in Ferroptosis. Mol Cell. 2019;73(2):354-63 e3.
858 58. Lewis SM, Williams A, Eisenbarth SC. Structure and function of the immune system
859 in the spleen. Science immunology. 2019;4(33).
860 59. Krüger-Genge A, Blocki A, Franke RP, Jung F. Vascular Endothelial Cell Biology: An
861 Update. Int J Mol Sci. 2019;20(18).
862 60. Dao M, MacDonald I, Asaro RJ. Erythrocyte flow through the interendothelial slits of
863 the splenic venous sinus. Biomechanics and modeling in mechanobiology.
864 2021;20(6):2227-45.
865 61. Mass E, Nimmerjahn F, Kierdorf K, Schlitzer A. Tissue-specific macrophages: how
866 they develop and choreograph tissue biology. Nature reviews Immunology.
867 2023:1-17.
868 62. Wen Y, Lambrecht J, Ju C, Tacke F. Hepatic macrophages in liver homeostasis and
869 diseases-diversity, plasticity and therapeutic opportunities. Cellular & molecular
870 immunology. 2021;18(1):45-56.
871 63. Li H, Lu L, Li X, Buffet PA, Dao M, Karniadakis GE, et al. Mechanics of diseased
872 red blood cells in human spleen and consequences for hereditary blood disorders.
873 Proc Natl Acad Sci U S A. 2018;115(38):9574-9.
874 64. Mebius RE, Kraal G. Structure and function of the spleen. Nature Reviews
875 Immunology. 2005;5(8):606-16.

878 ## Figure legends

879 **Fig.1 HH exposure promotes erythrocytosis in mice.** The C57BL/6 mice were
880 treated with normobaric normoxia (NN) and hypobaric hypoxia (HH) for 3, 7 and 14
881 days, and blood was collected for the following tests. (**A**) Analysis of the number and
882 morphology of RBCs via a blood cell smear. Routine blood analysis was performed
883 for RBC counts (**B**), as well as HGB (**C**), HCT (**D**), and MCH content (**E**). (**F**)
884 Representative dot plots (from three experiments) indicate TO-positive cells
885 (reticulocytes) in whole blood. Data are expressed as means ± SEM (n = 5 per group);
886 * $P < 0.05$, ** $P < 0.01$, *** $P < 0.001$ versus the NN group or the indicated group.

887

888 **Fig. 2 The spleen plays an important role in suppressing the immoderate increase**
889 **in RBCs under HH conditions.** C57BL/6 mice with or without splenectomy were
890 treated with NN and HH for varying durations, and the spleen and blood were
891 collected for subsequent analyses. (**A**) Morphological observation, (**B**) spleen volume,
892 and (**C**) spleen weight were determined post-HH exposure. (**D-H**) Blood observation
893 and hematological index detection followed. Data are expressed as the means ± SEM
894 (n = 9 per group); * $P < 0.05$, ** $P < 0.01$, *** $P < 0.001$ versus the NN group or the
895 indicated group.

896

897 **Fig. 3 HH exposure results in a decrease in the number of splenic macrophages.**
898 C57BL/6 mice were treated with NN and HH for 7 or 14 days, and the spleen and
899 blood were collected for subsequent detection. (**A**) Calcein/PI double staining was

900 analysed by flow cytometry. (**B and C**) The bar graphs represent cell death
901 proportions in total splenic cells. (**D**) Uniform manifold approximation and projection
902 (UMAP) visualized spleen cell clusters. Each color represents a cluster of specific
903 spleen cells, identified by a distinct gene expression profile. (**E**) The proportions of
904 different macrophage clusters derived from either NN- or HH-treated mouse spleens
905 were analysed. (**F**) Individual macrophages derived from either NN- or HH-treated
906 mouse spleens are denoted. (**G** and **J**) Western blot detecting CD16 and CD206
907 protein expression in the spleen. (**H-I** and **K-L**) Statistical analysis of CD16 and
908 CD206 expression in H and K. (**M**) F4/80 staining with CD11b, CD86 or CD206 in
909 splenic cells was analysed by flow cytometry. (**N**) qPCR analysis of CCL2 and CCL7
910 expression in the spleen. (**O**) qPCR analysis of Csf1 and Csf2 expression in the spleen.
911 (**P**) Flow cytometry detection of CD11b and Ly6C double-stained cells in the BM and
912 spleen. $CD11b^{hi}Ly6C^{hi}$ cell proportions in the BM (**Q-R**) and spleen (**S-T**) are given
913 as bar graphs. (**U**) HO-1 and F4/80 expression in the spleen after 0 (NN), 7, and 14
914 days of HH exposure. (**V**) The relative fluorescence of HO-1 and (**W**) F4/80
915 expression in the spleen as described in (U) was quantified. Data are expressed as the
916 means ± SEM (n = 3 per group); * $P < 0.05$, ** $P < 0.01$, *** $P < 0.001$ versus the
917 NN group or the indicated group.
918
919 **Fig. 4 HH exposure decreases erythrophagocytosis and iron processing capacity**
920 **in the spleen.** Flow cytometry revealed the proportion of FITC-stained cells in the
921 blood (**A**) and spleen (**B**) after 7 and 14 days of HH exposure. The proportions of

922 these FITC-positive cells in the blood (**C**) and spleen (**D**) are presented as bar graphs.
923 (**E**) Wright staining of splenic cells after HH exposure for 0 (NN), 7 and 14 days. (**F**)
924 The proportion of retention RBCs within the spleen cells. (**G**) Illustrating the
925 experimental design, in which C57BL6 mice (n=3 per group) were treated on days 7
926 and 11 with a single intravenous Tuftsin injection (1.5 mg/kg), followed by HH
927 exposure until day 14 for spleen isolation and subsequent F4/80
928 immunohistochemistry and iron staining. (**H**) F4/80 and iron staining in the spleen
929 after HH exposure for 14 days with Tuftsin treatment. (**I**) Quantitative the relative
930 fluorescence of F4/80 expression in the spleen described in (H). (**J**) Semiquantitative
931 iron levels in the spleen described in (H). Data are expressed as the means ± SEM (n
932 = 3 per group); * $P < 0.05$, ** $P < 0.01$, *** $P < 0.001$ versus the NN group or the
933 indicated group.
934
935 **Fig. 5 HH exposure promotes iron mobilization and induces ferroptosis in the**
936 **spleen.** The C57BL/6 mice were treated with NN and HH for 7 days, and the spleen
937 was collected for subsequent detection. (**A**) Western blot detection of HO-1, Ft-L,
938 Ft-H, NCOA4, Fpn and TfR protein expression in spleen. (**B**) Statistical analysis of
939 HO-1, Ft-L, Ft-H, NCOA4, Fpn and TfR protein expression. (**C**) GEO data analysis
940 of HMOX1, FTL, FTH1, NCOA4, SLC40A1, and TFRC mRNA expression in
941 PMBCs before and after climbing to high altitude (n=98). Western blot detection of
942 ACSL4, GPX4, and xCT protein expression in the spleen is shown in (**D**) and its
943 statistical analysis in (**E**). (**F**) GEO data analysis of ACSL4, GPX4 and SLC7A11

944 mRNA expression in PMBCs before and after reaching high altitude (n=98). (**G**) The
945 content of Fe^{2+} in the spleen was detected using the FerroFarRed probe by flow
946 cytometry. (**H**) The level of lipid ROS in the spleen was detected using the
947 C11-BODIPY probe by flow cytometry. The MDA (**I**), Cys (**J**) and GSH (**K**) levels in
948 the spleen were detected using biochemical detection kits, respectively. (**L**) Lillie
949 staining of Fe^{2+} in the spleen after 7 days of HH exposure. (**M**) Fe^{2+} deposition in the
950 spleen as described in (L) was quantified. Data are expressed as the means ± SEM (n
951 = 3 per group); * $P < 0.05$, ** $P < 0.01$, *** $P < 0.001$ versus the NN group or the
952 indicated group.
953
954 **Fig. 6 Hypoxia enhances primary peritoneal macrophage ferroptosis.** Primary
955 peripheral macrophages were cultured under 1% hypoxia for varying durations (0, 12,
956 24, 48 h), either with or without a pre-treatment of 10 μM Fer-1 for 1 h, before being
957 collected for further examination. (**A**) Immunofluorescence detection of Fe^{2+} levels in
958 macrophages after hypoxia exposure for 24 h using the FerroFarRed probe under a
959 fluorescence microscope. (**B**) Quantitative results of fluorescence intensity in the
960 macrophages described in A. (**C**) Flow cytometry detection of Fe^{2+} levels in
961 macrophages exposed to hypoxia for 24 h using the FerroFarRed probe. (**D**)
962 Immunofluorescence detection of lipid ROS levels in macrophages exposed to
963 hypoxia for 24 h using the C11-BODIPY probe under a fluorescence microscope. (**E**)
964 Quantitative results of mean fluorescence intensity in the macrophages described in D.
965 (**F**) Western blot detection of ACSL4, GPX4 and xCT protein expression in

macrophages under hypoxia for different times. (**G**) Flow cytometry was employed to analyze Calcein/PI double staining in macrophages following a 24 h hypoxia exposure. (**H**) Cell death proportions in macrophages are given as bar graphs. (**I**) Macrophage phagocytic activity against Cy5.5-labelled *E.coli* following 24 h of hypoxia exposure was assessed using flow cytometry *in vitro*. (**J**) Fe^{2+} levels in macrophages pre-treated with Fer-1, then exposed to 24 h of hypoxia, were detected via the FerroFarRed probe in immunofluorescence. (**K**) Quantitative results of fluorescence intensity in the macrophages described in J. (**L**) Western blot detection of ACSL4, GPX4 and xCT protein expression in macrophages pre-treated with Fer-1, then followed by 24 h of hypoxia exposure. (**M-O**) Statistical analysis of ACSL4, xCT, and GPX4 protein expression in L. MDA (**P**), Cys (**Q**), and GSH (**R**) levels in macrophages pre-treated with Fer-1 and subsequently exposed to 24 h of hypoxia were detected using kits and biochemical methods. Data are expressed as the means ± SEM (n = 3 per group); * $P < 0.05$, ** $P < 0.01$, *** $P < 0.001$ versus the NN group or the indicated group.

Fig. 7 High altitude/hypobaric hypoxia exposure suppresses erythrophagocytosis by inducing macrophages ferroptosis in the spleen. HA/HH exposure induces iron mobilization, especially increased Fe^{2+} levels, which are further increased in the spleen/macrophages of mice. On the other hand, HA/HH exposure increases ACSL4 expression, suppressing xCT expression and GSH production, which escalates lipid peroxidation and subsequent macrophage ferroptosis. Meanwhile, HA/HH exposure

988 decreases monocyte migration and differentiation from the BM to the spleen. Taken
989 together, HA/HH exposure inhibits erythrophagocytosis and further promotes
990 erythrocytosis, which may aggravate HAPC development.
991
992
993 **Supplementary Figure S1. HH exposure promotes iron mobilization and induces**
994 **ferroptosis in the spleen.** The C57BL/6 mice were treated with NN and HH for 14
995 days, and the spleen was collected for subsequent detection. (**A**) Western blot
996 detection of HO-1, Ft-L, Ft-H, NCOA4, Fpn and TfR protein expression in spleen. (**B**)
997 Statistical analysis of HO-1, Ft-L, Ft-H, NCOA4, Fpn and TfR protein expression in
998 **A**. (**C**) Western blot detection of ACSL4, GPX4 and xCT protein expression in the
999 spleen. (**D**) Statistical analysis of ACSL4, GPX4 and xCT protein expression in **C**. (**E**)
1000 The content of Fe^{2+} in the spleen was detected using the FerroFarRed probe by flow
1001 cytometry. (**F**) Quantitative results of the mean fluorescence intensity in **E**. (**G**) The
1002 level of lipid ROS in the spleen was detected using the C11-BODIPY probe by flow
1003 cytometry. (**H**) Quantitative results of the mean fluorescence intensity in **G**. (**I**) MDA,
1004 (**J**) Cys, and (**K**) GSH levels in the spleen were detected using kits by biochemical
1005 methods. (**L**) Lillie staining of Fe^{2+} in the spleen after 14 days of HH exposure. (**M**)
1006 Fe^{2+} deposition in the spleen as described in (L) was quantified. Data are expressed as
1007 the means ± SEM (n = 3 per group); * $P < 0.05$, ** $P < 0.01$, *** $P < 0.001$ versus the
1008 NN group or the indicated group.

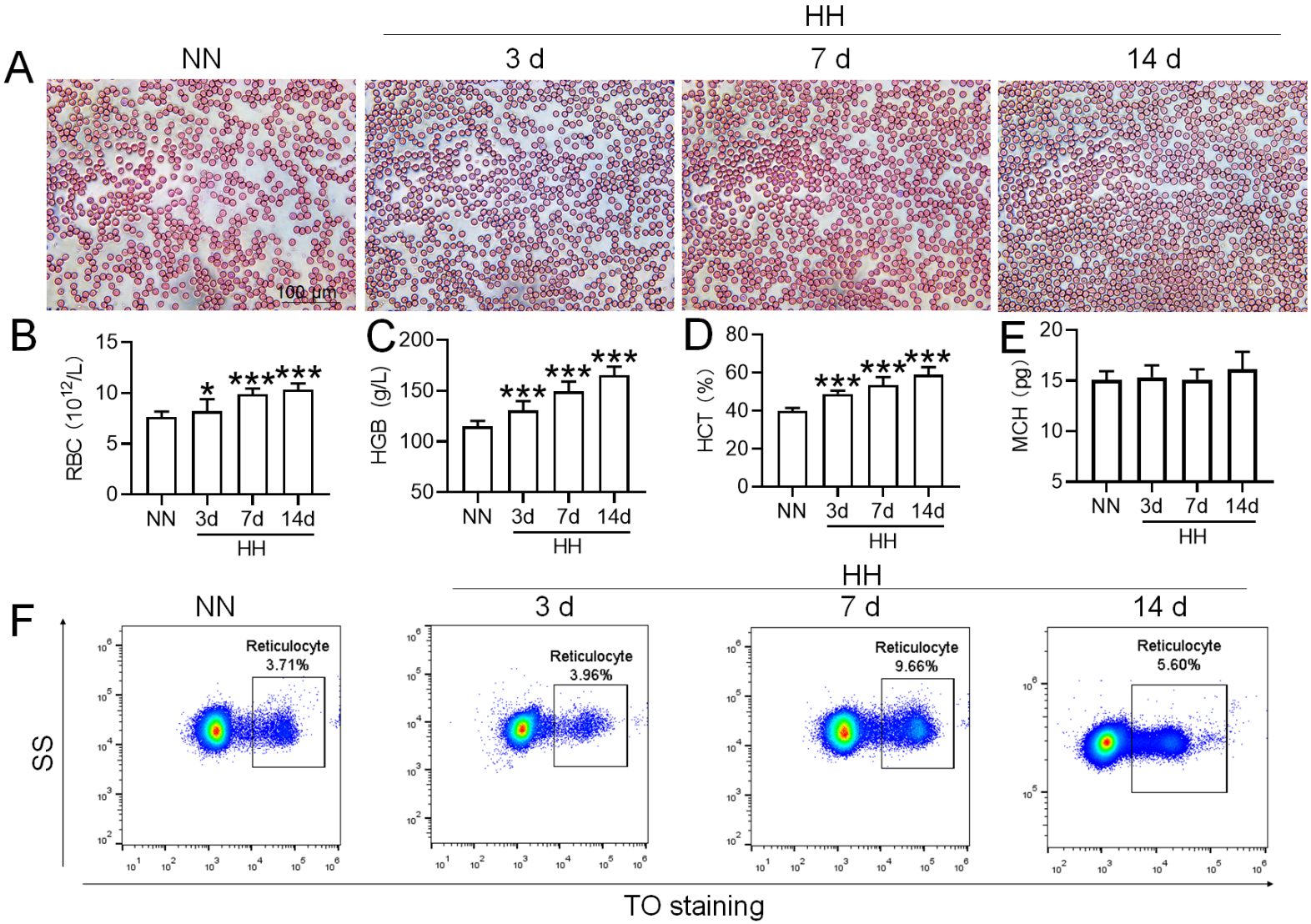
A
NN
HH
3 d
7 d
14 d
100 μm
B
RBC (10^12/L)
C
HGB (g/L)
D
HCT (%)
E
MCH (pg)
NN
3d
7d
14d
HH
F
Reticulocyte
3.71%
3.96%
9.66%
5.60%
SS
TO staining

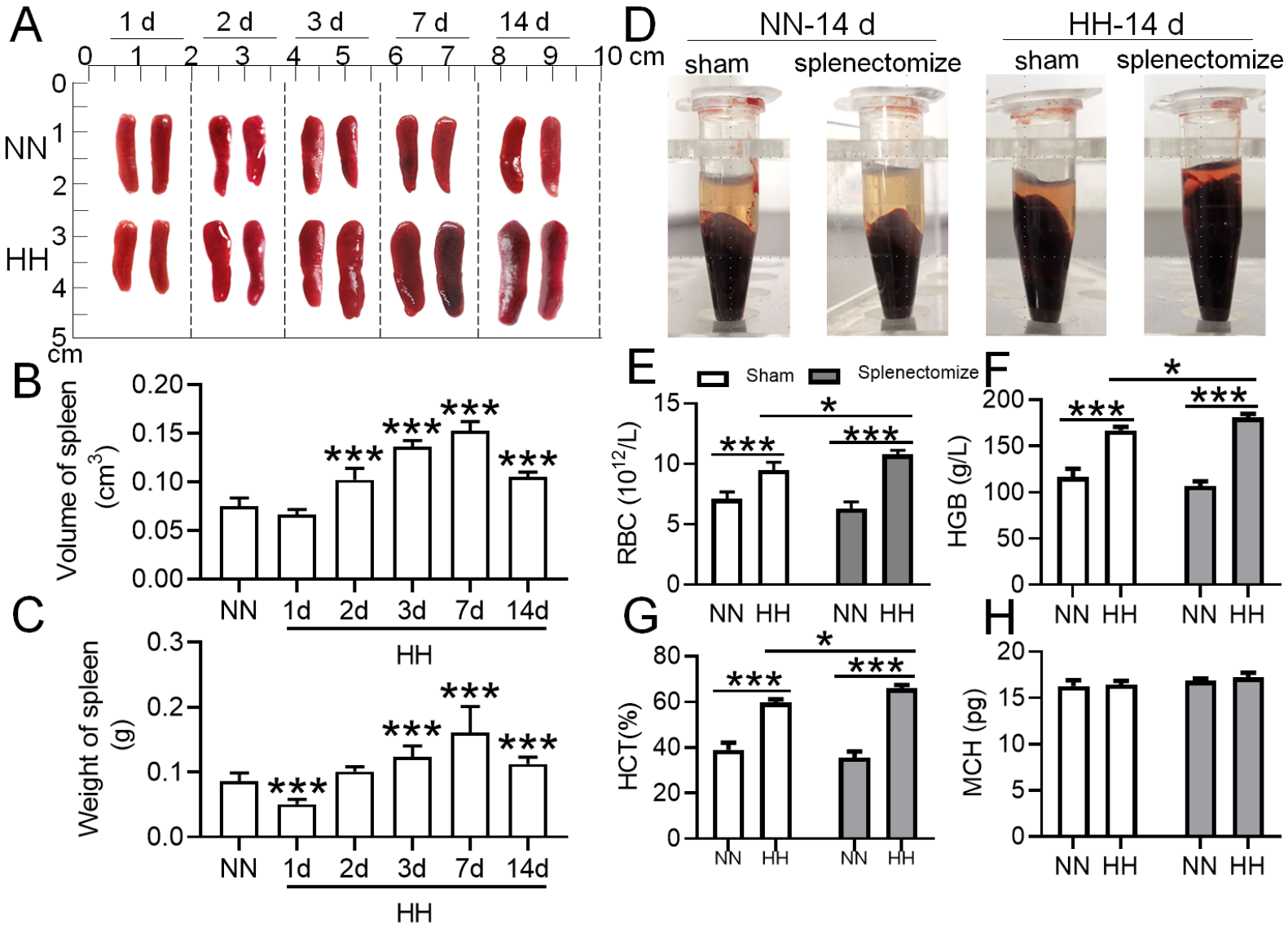
A
1 d
2 d
3 d
7 d
14 d
0 1 2 3 4 5 6 7 8 9 10 cm
NN
HH
cm
B
Volume of spleen (cm3)
0.20
0.15
0.10
0.05
0.00
***
NN 1d 2d 3d 7d 14d
HH
C
Weight of spleen (g)
0.3
0.2
0.1
0.0
NN 1d 2d 3d 7d 14d
HH
D
NN-14 d
HH-14 d
sham
splenectomize
sham
splenectomize
E
Sham
Splenectomize
RBC (10^12/L)
15
10
5
0
*
***
NN HH NN HH
F
HGB (g/L)
200
150
100
50
0
G
HCT(%)
80
60
40
20
0
H
MCH (pg)
20
15
10
5
0

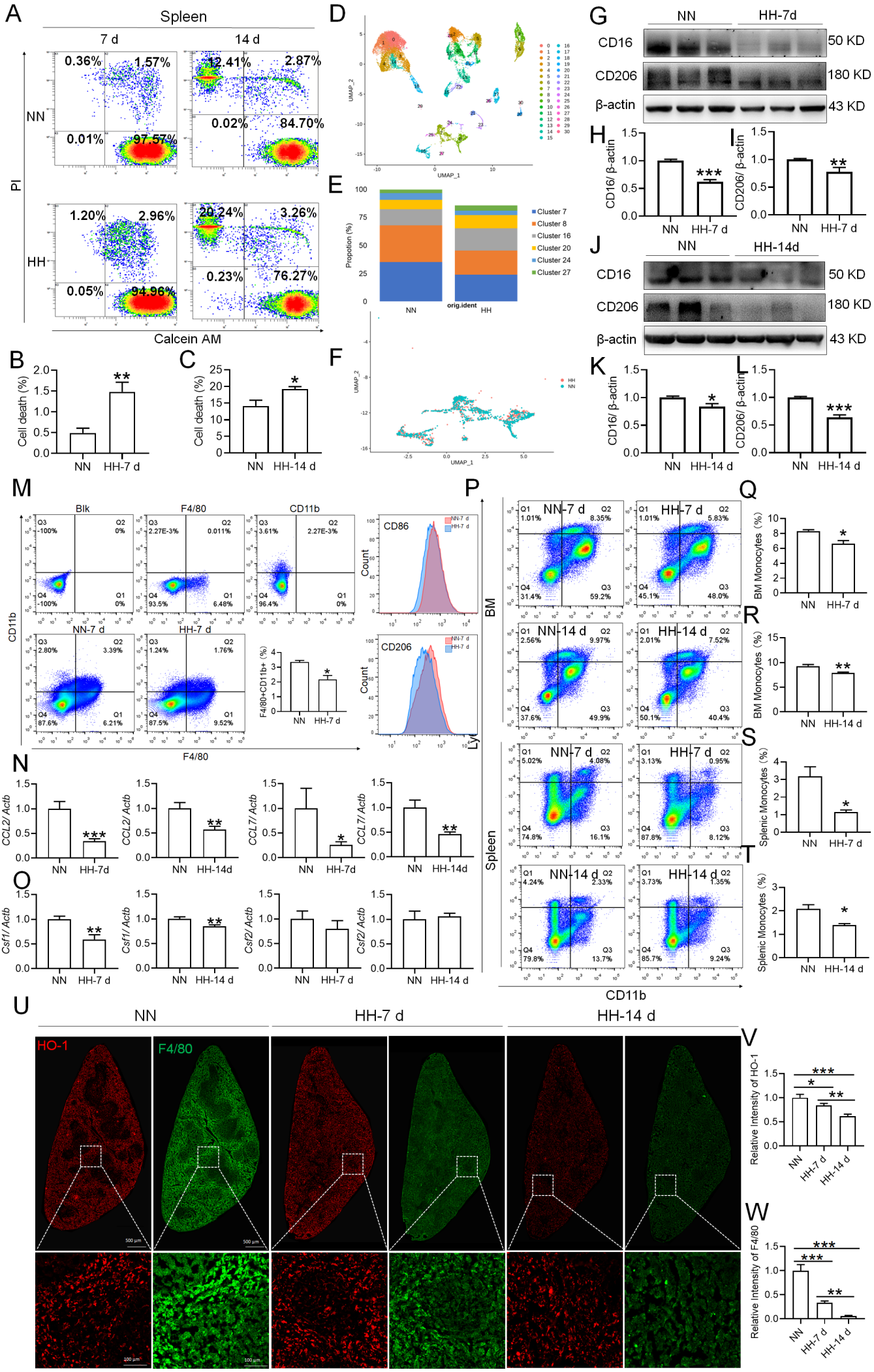
A
Spleen
7 d
14 d
NN
HH
PI
Calcein AM
0.36%
1.57%
0.01%
97.57%
12.41%
2.87%
0.02%
84.70%
1.20%
2.96%
0.05%
94.96%
20.24%
3.26%
0.23%
76.27%
B
Cell death (%)
NN
HH-7 d
C
Cell death (%)
NN
HH-14 d
D
UMAP_1
UMAP_2
E
Propotion (%)
Cluster 7
Cluster 8
Cluster 16
Cluster 20
Cluster 24
Cluster 27
orig.ident
NN
HH
F
UMAP_1
UMAP_2
HH
NN
G
NN
HH-7d
CD16
CD206
β-actin
50 KD
180 KD
43 KD
H
CD16/ β-actin
NN
HH-7 d
I
CD206/ β-actin
NN
HH-7 d
J
NN
HH-14d
CD16
CD206
β-actin
50 KD
180 KD
43 KD
K
CD16/ β-actin
NN
HH-14 d
L
CD206/ β-actin
NN
HH-14 d
M
Blk
F4/80
CD11b
NN-7 d
HH-7 d
CD11b
F4/80
F4/80+CD11b+ (%)
NN
HH-7 d
CD86
CD206
Count
Ly
N
CCL2/ Actb
CCL7/ Actb
NN
HH-7d
HH-14d
O
Csf1/ Actb
Csf2/ Actb
NN
HH-7 d
HH-14 d
P
BM
Spleen
NN-7 d
HH-7 d
NN-14 d
HH-14 d
CD11b
Q
BM Monocytes (%)
NN
HH-7 d
R
BM Monocytes (%)
NN
HH-14 d
S
Splenic Monocytes (%)
NN
HH-7 d
T
Splenic Monocytes (%)
NN
HH-14 d
U
NN
HH-7 d
HH-14 d
HO-1
F4/80
500 μm
100 μm
V
Relative Intensity of HO-1
NN
HH-7 d
HH-14 d
W
Relative Intensity of F4/80
NN
HH-7 d
HH-14 d

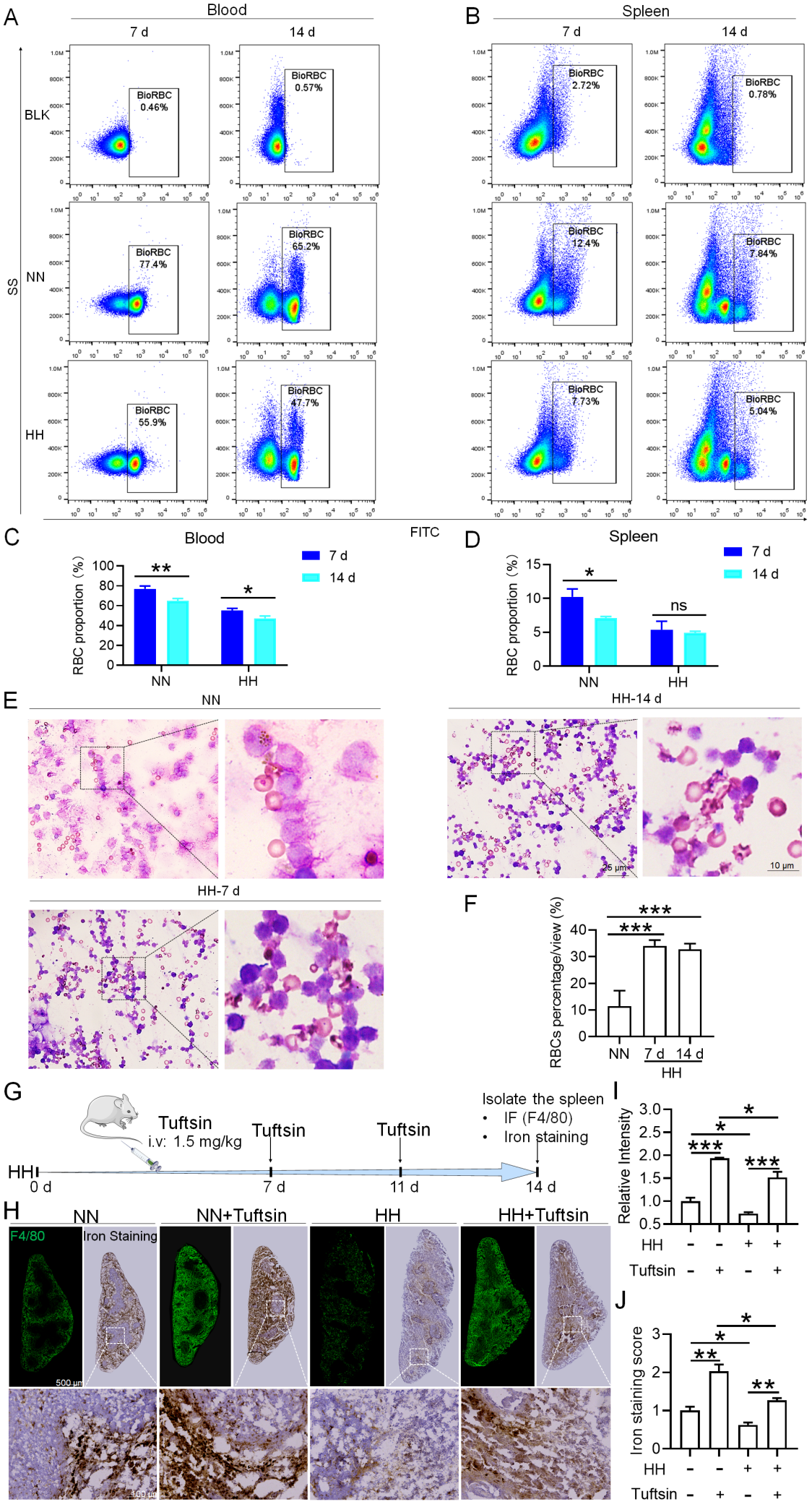
A
Blood
7 d
14 d
BLK
NN
HH
SS
FITC
BioRBC 0.46%
BioRBC 0.57%
BioRBC 77.4%
BioRBC 65.2%
BioRBC 55.9%
BioRBC 47.7%
B
Spleen
BioRBC 2.72%
BioRBC 0.78%
BioRBC 12.4%
BioRBC 7.84%
BioRBC 7.73%
BioRBC 5.04%
C
Blood
RBC proportion (%)
7 d
14 d
NN
HH
D
Spleen
ns
E
NN
HH-14 d
HH-7 d
25 μm
10 μm
F
RBCs percentage/view (%)
G
Tuftsin
i.v: 1.5 mg/kg
Isolate the spleen
IF (F4/80)
Iron staining
0 d
7 d
11 d
14 d
H
NN
NN+Tuftsin
HH
HH+Tuftsin
F4/80
Iron Staining
500 μm
100 μm
I
Relative Intensity
Tuftsin
J
Iron staining score

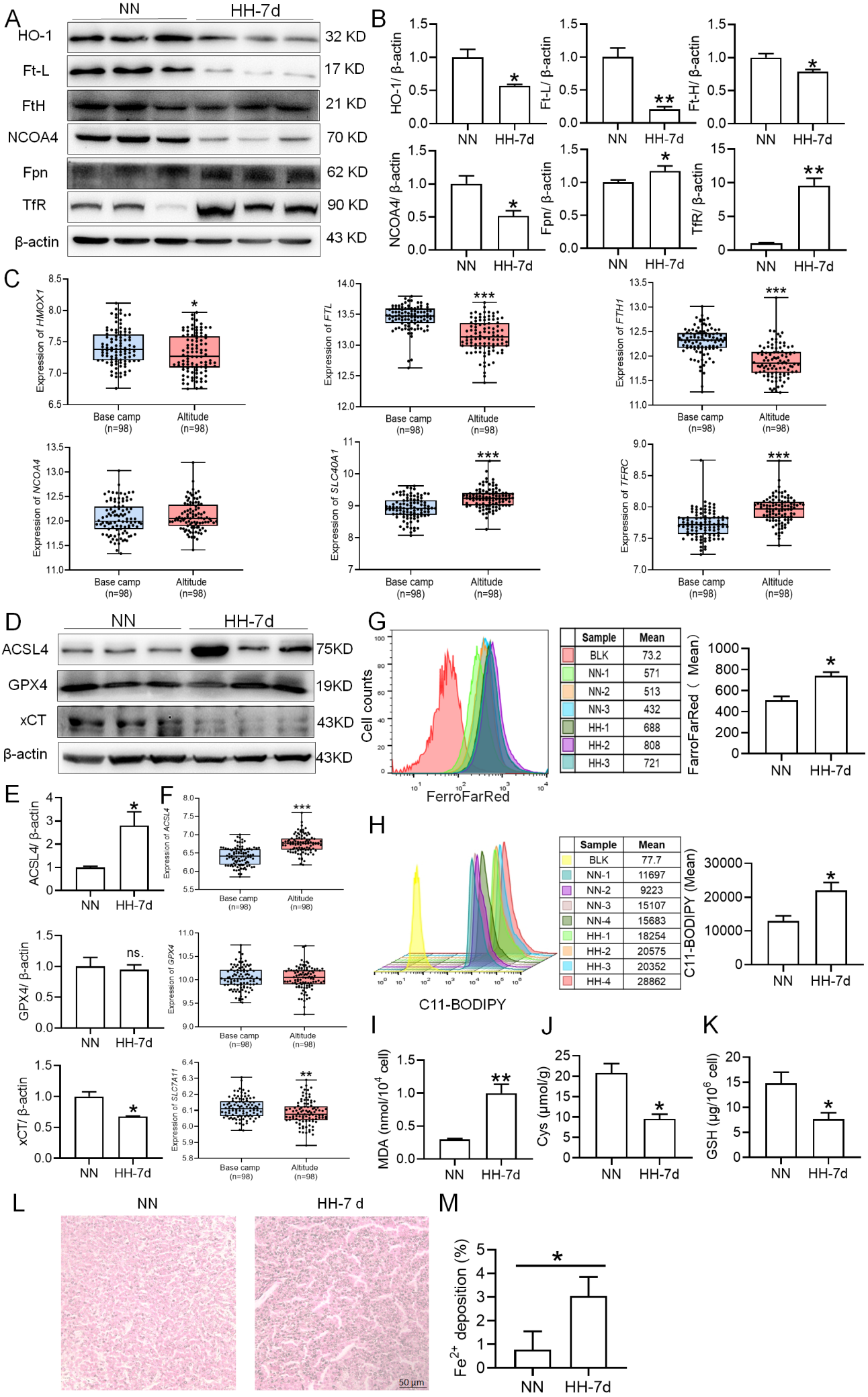
A
NN
HH-7d
HO-1
Ft-L
FtH
NCOA4
Fpn
TfR
β-actin
32 KD
17 KD
21 KD
70 KD
62 KD
90 KD
43 KD
B
HO-1/ β-actin
Ft-L/ β-actin
Ft-H/ β-actin
NCOA4/ β-actin
Fpn/ β-actin
TfR/ β-actin
NN
HH-7d
C
Expression of HMOX1
Expression of FTL
Expression of FTH1
Expression of NCOA4
Expression of SLC40A1
Expression of TFRC
Base camp (n=98)
Altitude (n=98)
D
ACSL4
GPX4
xCT
β-actin
75KD
19KD
43KD
43KD
E
ACSL4/ β-actin
GPX4/ β-actin
xCT/ β-actin
ns.
F
Expression of ACSL4
Expression of GPX4
Expression of SLC7A11
G
Cell counts
FerroFarRed
FarroFarRed（Mean）
Sample | Mean
BLK | 73.2
NN-1 | 571
NN-2 | 513
NN-3 | 432
HH-1 | 688
HH-2 | 808
HH-3 | 721
H
C11-BODIPY
C11-BODIPY (Mean)
Sample | Mean
BLK | 77.7
NN-1 | 11697
NN-2 | 9223
NN-3 | 15107
NN-4 | 15683
HH-1 | 18254
HH-2 | 20575
HH-3 | 20352
HH-4 | 28862
I
MDA (nmol/10^4 cell)
J
Cys (μmol/g)
K
GSH (μg/10^6 cell)
L
NN
HH-7 d
50 μm
M
Fe2+ deposition (%)

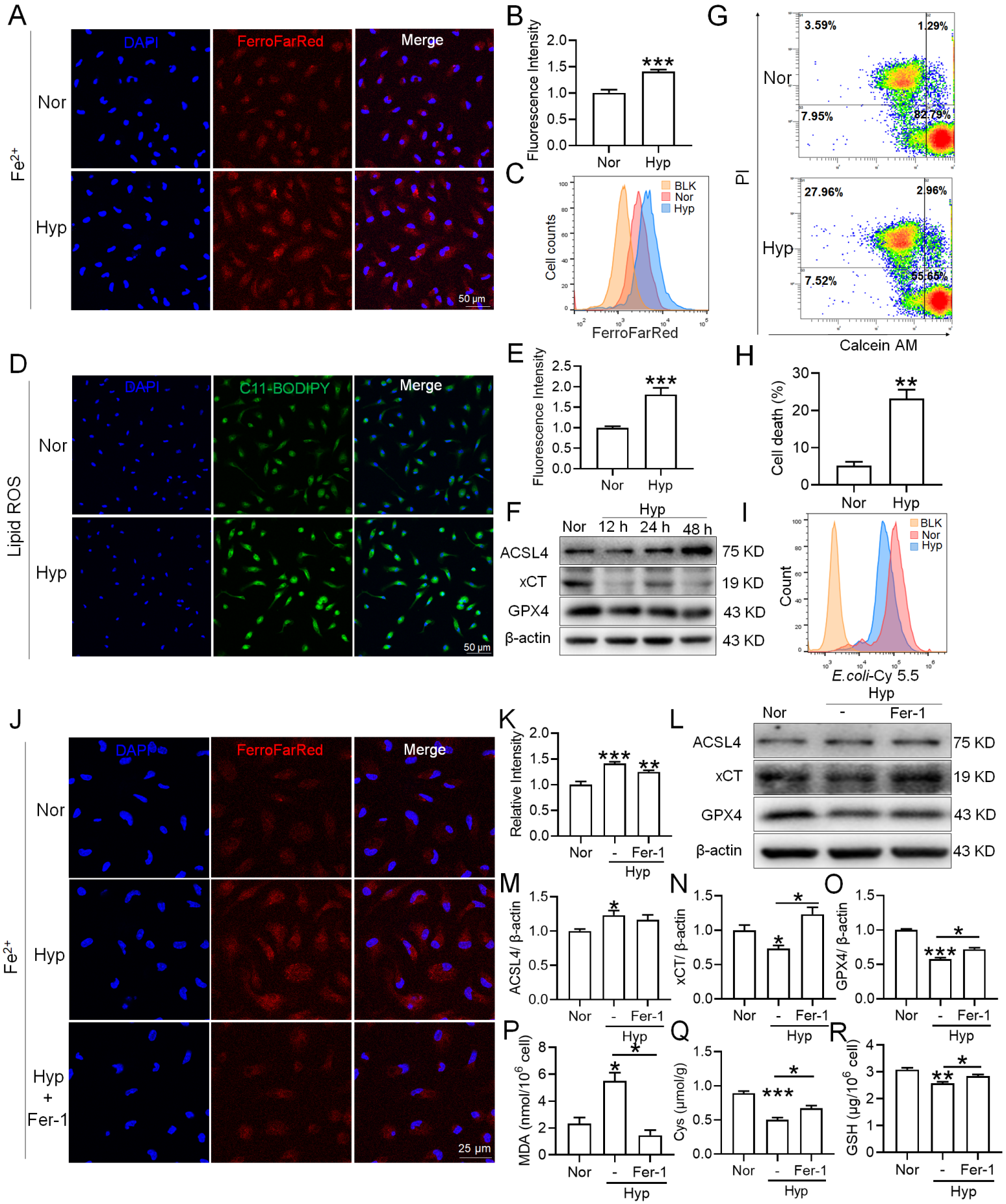
A
DAPI
FerroFarRed
Merge
Nor
Hyp
Fe2+
50 μm
B
Fluorescence Intensity
Nor
Hyp
C
BLK
Nor
Hyp
Cell counts
FerroFarRed
G
3.59%
1.29%
7.95%
82.79%
27.96%
2.96%
7.52%
55.65%
PI
Calcein AM
D
DAPI
C11-BODIPY
Merge
Lipid ROS
50 μm
E
Fluorescence Intensity
H
Cell death (%)
F
Nor
12 h
24 h
48 h
Hyp
ACSL4
xCT
GPX4
β-actin
75 KD
19 KD
43 KD
43 KD
I
BLK
Nor
Hyp
Count
E.coli-Cy 5.5
J
DAPI
FerroFarRed
Merge
Nor
Hyp
Hyp + Fer-1
Fe2+
25 μm
K
Relative Intensity
Fer-1
L
ACSL4
xCT
GPX4
β-actin
75 KD
19 KD
43 KD
43 KD
M
ACSL4/ β-actin
N
xCT/ β-actin
O
GPX4/ β-actin
P
MDA (nmol/10^6 cell)
Q
Cys (μmol/g)
R
GSH (μg/10^6 cell)

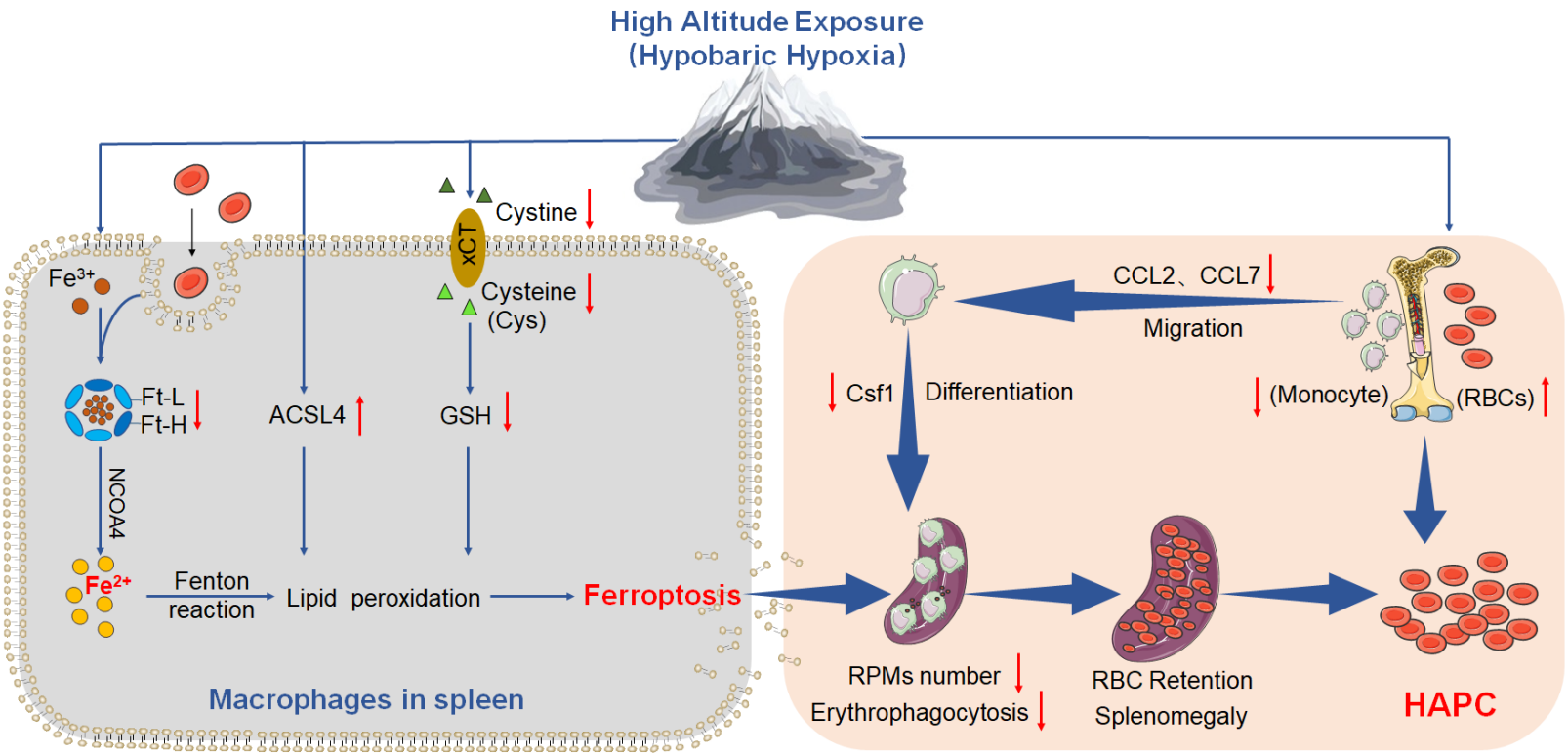
High Altitude Exposure
(Hypobaric Hypoxia)
Cystine
xCT
Cysteine
(Cys)
Fe3+
Ft-L
Ft-H
ACSL4
GSH
NCOA4
Fe2+
Fenton
reaction
Lipid peroxidation
Ferroptosis
Macrophages in spleen
CCL2、CCL7
Migration
Csf1
Differentiation
(Monocyte)
(RBCs)
RPMs number
Erythrophagocytosis
RBC Retention
Splenomegaly
HAPC